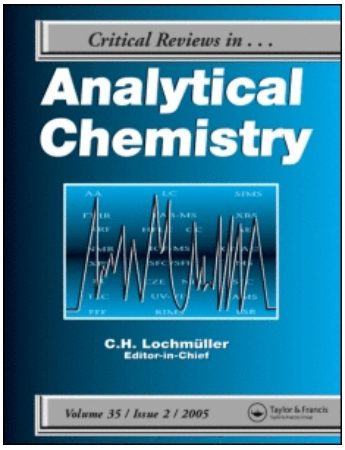

Critical Reviews in Analytical Chemistry
Publication details, including instructions for authors and subscription information:
http://www.informaworld.com/smpp/title~content=t713400837

A Model for Mechanism of Peroxyoxalate Chemiluminescence as Applied to Detection in Liquid Chromatography

György Orosz[a]; Richard S. Givens[b]; Richard L. Schowen[b]
[a] Research Group of Peptide Chemistry, Eötvös Loránd University, Budapest 112, Hungary [b] Center for BioAnalytical Research (Higuchi Biosciences Centers) and the Department of Chemistry, University of Kansas, Lawrence, KS

To cite this Article Orosz, György , Givens, Richard S. and Schowen, Richard L.(1996) 'A Model for Mechanism of Peroxyoxalate Chemiluminescence as Applied to Detection in Liquid Chromatography', Critical Reviews in Analytical Chemistry, 26: 1, 1 — 27
To link to this Article: DOI: 10.1080/10408349608050566
URL: http://dx.doi.org/10.1080/10408349608050566

Critical Reviews in Analytical Chemistry, 26(1):1–27 (1996)

A Model for Mechanism of Peroxyoxalate Chemiluminescence as Applied to Detection in Liquid Chromatography

György Orosz,[1] Richard S. Givens,[2] and Richard L. Schowen[2]*

[1]Research Group of Peptide Chemistry, Eötvös Loránd University, P.O. Box 32, Budapest 112, H-1518 Hungary; [2]Center for BioAnalytical Research (Higuchi Biosciences Centers) and the Department of Chemistry, University of Kansas, Lawrence, KS 66045-0046

* Author to whom all correspondence should be addressed.

ABSTRACT: In recent years, a substantial body of knowledge has been accummulated on the mechanism of peroxyoxalate chemiluminescence (PO-CL). Formal mechanisms have been reported previously by the authors and others purporting to account for the effects of variation of the primary reagents (concentration of oxalate, hydrogen peroxide, and fluorophore) on the peroxyoxalate induced detection of analytes in liquid chromatography and flow injection analyses. In this article, new pathways are suggested also for the induced decomposition of the chemiluminescent intermediate, including: (a) its reaction with a quencher, and (b) its reaction with hydrogen peroxide. Quantitative relationships are derived and established for the effect of pH on the maximum light intensity and the rate of the light decay. The parameters extracted from the experimental data are utilized to predict the influence of reagent concentrations and flow rates on the chemiluminescent detector response. In contrast to the linearity of the relationships in the static solution studies, significant nonlinearities are presented, based on simulations of experimental conditions for flow systems. Among the several conclusions reached, the most important is that the location of the maximum chemiluminescent response in flow systems may not be accomplished by simply determining the optimal values for the individual parameters.

KEY WORDS: peroxyoxalate, chemiluminescence detection, modeling.

I. INTRODUCTION

Since its discovery, peroxyoxalate chemiluminescence (PO-CL) (i.e., the reaction of an oxalate and hydrogen peroxide in the presence of fluorescent molecule to generate light) has been a significant mechanistic and theoretical challenge. Interest in this reaction is driven by the successful application of the chemiluminescent reaction to a variety of analytical problems:

1. Quantitative determination of certain fluorescent analytes in which separations are achieved by TLC [1,2], capillary electrophoresis [3,4], supercritical fluid chromatography [5], the determination by liquid chromatography [6–22]

1040-8347/96/$.50

through either pre- or postcolumn derivation of nonfluorescent analytes [13,17,23–29] and by several types of flow injection analyses [40–48]

2. Quantitative analysis of hydrogen peroxide [42,44,49–53] generated enzymatically or in enzyme immunoassays [64–66]
3. Determination of oxalic acid [67, 68]
4. Quantitation of phenols through the formation of oxalates [69, 70]
5. Determination of analytes capable of quenching the PO-CL reaction [40,43, 71–74]
6. Analysis of compounds that enhance the chemiluminescence [75–78] or the background emission [79]

In this article, we attempt to demonstrate that a working hypothetical mechanism is available that can be applied to derive quantitative relationships to guide the practitioner in optimizing the use of PO-CL for high-performance liquid chromatography (HPLC) and flow injection analyses.

The model incorporates several important features from the earlier modeling efforts, and can be viewed as a critical reevaluation of the known mechanistic approaches and experimental data.

The PO-CL–based detection is affected by several instrumental parameters (i.e., reagent and eluent flows, concentrations) [6,8,80–82]; many of them are hardly controlled if controlled at all, (e.g., detector geometry and volume [83,84], pump pulsation [16], the mixing of the reagent and eluent flows [22,85–87], or background emission [5,15,77,88–91]).

Without a reliable mechanistic basis, it is difficult to distinguish between the effects due to the change in instrumental parameters and the factors affecting the mechanism, but even without the detailed mechanistic background, the PO-CL reaction has been successfully utilized in sensitive assays [1,2,54–57,92,93].

It took some time before it was realized that light intensity decays recorded in the static experiments could be utilized as good starting points for fine-tuning the dynamic systems [94]. Since then, static modeling has been an indispensable tool for studying the effects of the individual components (e.g., solvent composition, pH, reagent concentrations, additives, etc.) [40,64,83,95–100].

A more accurate approximation of the light intensity-time curve by an exponential decay and characterization of the curve by an exponential decay and characterization of the light intensity-time curve by the maximal light intensity and the half-life of the light intensity was another important step in the description of the PO-CL phenomenon. An elegant demonstration for the application of the static method is the prediction of the detection limits in flow systems based on the data collected in static experiments [10].

The exponential approximation of the light intensity-time curve was the basis of the first model developed by de Jong and his co-workers [83,101], who described the response of the PO-CL–based detector. In the first version of the "time-window" concept [102], it was assumed that the detector captures and integrates that part of the exponential light decay taking place inside the detector. Thus, a determination of the delay time between the point where the reagents are mixed and the entrance of the sample into the detector, along with the time interval during which the light is captured by the detector could be manipulated to obtain the chemiluminescence response based upon the data obtained from static experiments [101]. In certain cases, this model behaved well, whereas in others it gave unreliable values for the detector response. By now the explanation is obvious: in the description of the chemiluminescent decay, the initial stage (when the chemiluminescence signal increases) was ignored [82].

In mixed organic solvent-buffer mixtures, the kinetics of the light emission is greatly

simplified. Stopped-flow determinations allowed an accurate description of the entire light emission curve [102,103]. The integrated light intensities obtained from these determinations correlated nicely with the experimental values, and led to the explicit formulation of the "time-window" concept [102].

More rigorous investigations of the stopped-flow data revealed that under strictly controlled and well-defined conditions, the shape of the light intensity decay can be approximated accurately by a biexponential function [104].

The parameters obtained from the experimental data are suitable for quantitative mechanistic studies. The data generated by Orlovic [104] served as starting points in developing the model being presented.

In this article, in contrast to the earlier modeling attempts where only the kinetics of the light emission were utilized to predict the chemiluminescent response, the parameters describing the PO-CL light emission are obtained directly from a reaction mechanism. In this way, the deduced and the experimental parameters can be compared, the validity of the deduced expressions can be checked, and thus, the behavior of the chemiluminescent system can be quantitatively evaluated. Consequently, on the basis of the data obtained from the static chemiluminescent measurements, the model is capable of describing the trends in the chemiluminescent system. It further provides an approach to the determination of the maximum chemiluminescent response by changing the parameters in a systematic optimization protocol [7,100].

II. KINETICS AND LIQUID CHROMATOGRAPHIC DETECTION

To determine the concentration of the analyte by chemiluminescence detection, it is important to recall that the signal observed at the detector is a function of the rates and efficiencies of the chemical light generation process. In a study on the kinetic parameters for a chemiluminescent reaction, a static solvent system has the advantage of having fewer variables; therefore, the determination of parameters requires fewer steps. The primary purpose of this work is to demonstrate how these data can be used to determine the initial points in the optimization of the flow system and how the data obtained from these experiments may be interpreted.

A typical light intensity-time curve (I_t) for the PO-CL reaction in static experiments is shown in Figure 1. This curve can be usefully approximated by the expression [104]

$$I_t = K \cdot (e^{-f \cdot t} - e^{-r \cdot t}) \qquad (1)$$

where t is the time, and K is a constant dependent on the microscopic rate constants f and r for the reactions generating and destroying the activator. r describes the rise rate before the maximum light intensity J is reached, whereas f is the corresponding exponential fall rate. Because the rise of the light intensity is much faster than that of the fall, this expression can be simplified to an exponential decay form [101,105–107] for the major part of the reaction profile:

$$I_t = I_0 \cdot e^{-f \cdot t} \qquad (2)$$

where I_0 is the hypothetical light intensity at the maximum (J). In static experiments, the most frequently reported parameters are the maximum peak intensity (J) and the rate of the pseudo-first–order light decay (f).

To apply the kinetic data obtained from the static solution studies to chemiluminescence detection, it is necessary to assume that the reaction proceeds in the same way in the flow system as it does in the static solution experiments. As to the extent to which the reaction is completed within the residence time in the detector, (e.g., the ratio of

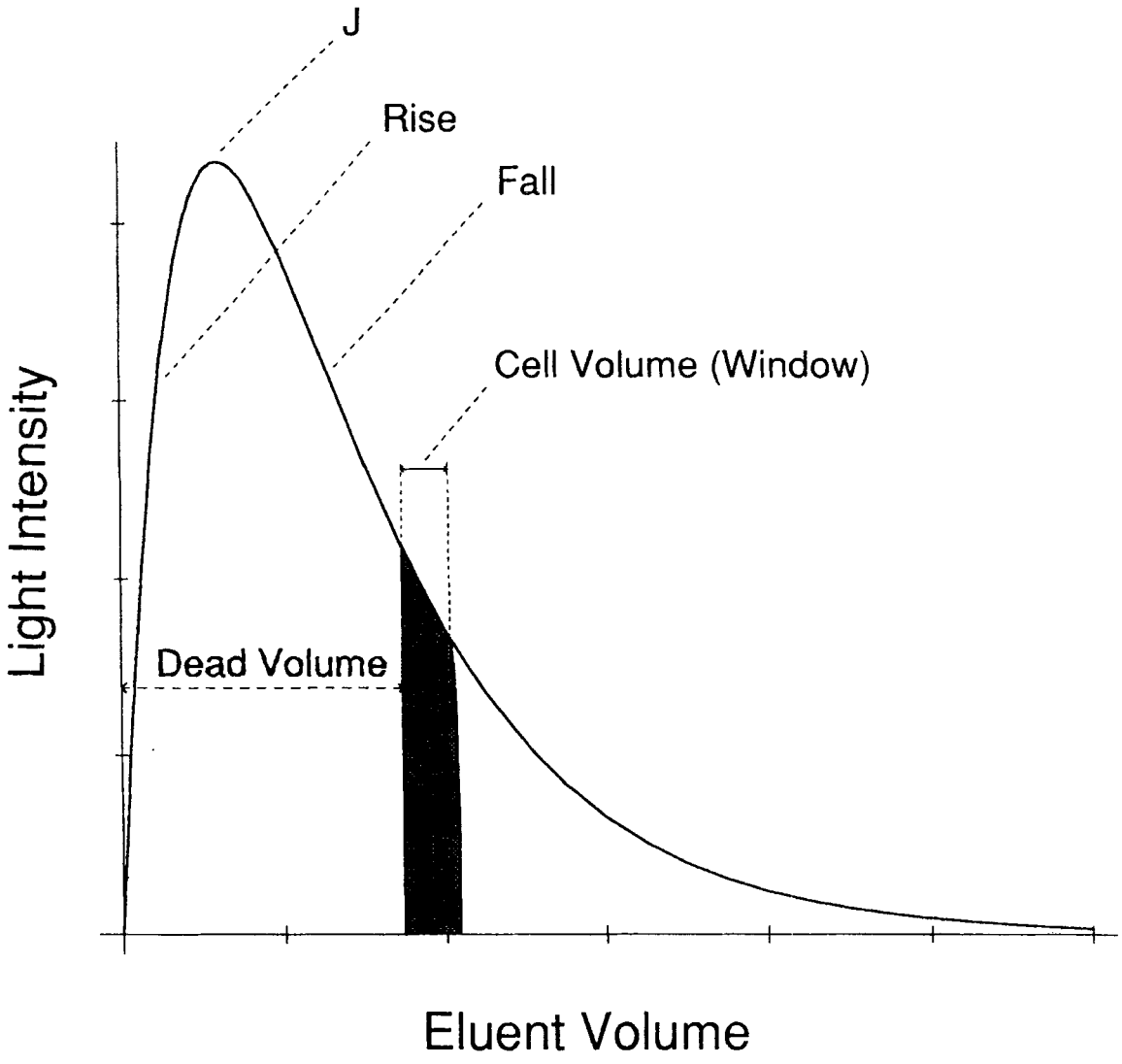

FIGURE 1. Typical light intensity-time decay curve and its connection with the chemiluminescent detector. The detector views a certain part of the reaction determined by the cell volume.

the half-life of the reaction to the residence time of reaction mixture in the detector), two limiting situations can be designated:

1. When the half-life of the reaction is very short compared with the residence time, the major portion of the chemiluminescence emission will occur inside the detector cell. This condition is designated as the "integrating" detector because the response is roughly proportional to the number of photons emitted from the reaction mixture (L_e), and therefore is equivalent to the quantum efficiency in the static experiments. Assuming that there is no significant dead volume after the mixing point, the detector is only sensitive to the factors affecting the quantum efficiency.
2. When the half-life of the reaction is much longer than the residence time, a fraction of the total emitted light arrives

inside the detector cell. This detector is termed a differential detector, and its response will be proportional to the light intensity (I_t) in the static experiments represented by the integrated portion of the time/intensity profile during the residence period in the cell (see Figure 1). With this type of detector, a dead volume must exist between the mixing point and the detector because there is no light intensity measured at the moment of mixing (Figure 1). This dead volume basically determines the chemiluminescent response. It has an optimal value corresponding to the volume that passes through the cell before the light emission reaches maximum intensity (J, Figure 1).

The "time-window" concept [102] has been applied successfully to approximate the chemiluminescent signal collected in the detector (Figure 1) from these two configurations. Our attention in this article will be focused on the differential detector because most of the systems can be sufficiently approximated by this model. The experimental verification of the influence of different cell volumes on the chromatographic performance was established by de Jong [83,101] and Cepas et al. [90].

III. A MODEL FOR THE PEROXYOXALATE-BASED DETECTION

In the optimization of the analytical system, the primary purpose is to vary the system's parameters and adjust the kinetics of the PO-CL reaction to obtain the maximum signal with minimum noise at the detector. The adjustment of the PO-CL reaction kinetics may be accomplished in numerous ways (e.g., using different oxalates, varying the reagents and concentrations, changing the eluent [95] and reagent flow rates [15,29,31], using different solvents, pH, acidic or basic additives, catalysts [7,76,102–104,108,109], surfactants [61,110,111], metal ions [99], etc.).

Most applications of the PO-CL reaction make use of organic solvent-buffer mixtures to control the pH and to assure adequate solubility of all of the reagents. Buffers, however, may add complications by influencing the rates of the PO-CL reaction with respect to the competing oxalate hydrolysis [107,112–115]. The exact role of a buffer and of other such additives is largely unknown and has been investigated in few cases only [15,29,51,76,102–104,108,115,116]. In determining the optimum PO-CL conditions, however, these factors have been considered to be "minor" effects despite their occasional controlling influence on the kinetics of the reaction [102], whereas the principal components of the PO-CL reaction — the oxalate, hydrogen peroxide, and fluorophore — are treated as primary determining components.

In spite of the numerous factors affecting the reaction rate, it has been shown that the light emission in these systems can be satisfactorily described by the simple mathematical formula [104] shown in Equation 1. The complex mechanisms proposed earlier [72,104–107,116–119] were based on kinetic and physicochemical measurements under different circumstances. The complex kinetic system for the mechanism in nonaqueous media proposed by Catherall et al. [105,106] can be integrated successfully by assuming steady-state concentrations of the key intermediates.

In this study, the Palmer Cundall and Catherall model is expanded to account for the influence of the additional contributing steps in organic solvent-buffer media (Scheme 1). The first (and, in this treatment, the rate-determining) step is the reaction of the oxalate with a buffer-hydrogen peroxide mixture. This kind of reaction includes hydrolysis [107,112–114] (Reaction 1), reaction with hydrogen peroxide yielding the chemiluminescent intermediate (Reaction 2),

and side reactions (Reaction 3). (Although intermediate X itself is not chemiluminescent, it is merely responsible for activating a fluorophore to its fluorescent state; nevertheless, for simplicity it will be termed here as a chemiluminescent intermediate.) Reaction 3 expresses a strong dependence of the light production on the structure of oxalate [29,51,96,97,107,120].

The chemiluminescent intermediate (or intermediates) [107,117,121] X in this approach has a structure resembling the starting oxalate either in the form of a dioxetane [105–107], a hydroperoxyoxalate [118], or acyl–peroxyoxalate [116]. The intermediate [121] is thought to be unstable under the harsh conditions of PO-CL detection, (i.e., its decomposition rate is faster than the rate of its formation) [105–107].

X is partitioned through its decomposition by the unimolecular reaction (4), reactions with the fluorophore (F) to form a complex (XF) (5), or quenching (6). The reactions of X with the fluorophore and quencher (Q) are thought to follow the CIEEL mechanism proposed by Schuster [122]. Therefore, X is expected to react faster with the quencher, which has a lower oxidation potential than with the fluorophore.

An additional pathway for the decomposition of X is the reaction with hydrogen

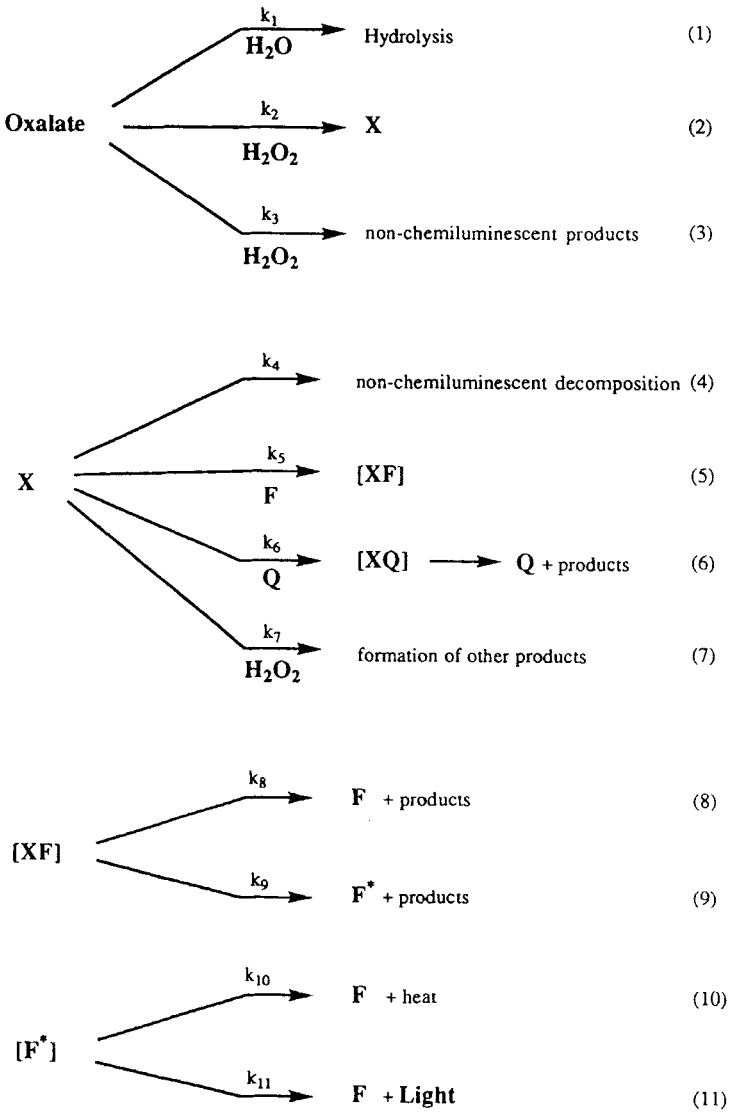

peroxide (7) to yield possibly the diperoxyoxalic acid (a known and relatively stable compound) [123], as suggested earlier by Rauhut [119].

The decomposition of the fluorophore-intermediate complex (XF) partitions through pathway 8 or by excitation of the fluorophore (9). Fluorophores that have less than unit quantum efficiencies lead to additional losses in energy (10,11).

A. Kinetic Treatment of the Mechanism

Application of a steady-state concentration for each of the intermediates is used to solve the complex mechanism formulated in Scheme 1 for the static PO-CL system. The concentration of the oxalate can be approximated under pseudo first-order conditions for the oxalate as

$$[\text{oxalate}] = [\text{oxalate}]_0 \cdot e^{(k_1 \cdot [H_2O] + (k_2 + k_3) \cdot [H_2O_2]) \cdot t} \quad (3)$$

where $[\text{oxalate}]_0$ and [oxalate] are the oxalate concentrations at the beginning of the reaction and after the time t, respectively. Assuming steady-state concentrations for intermediates X, XF, and F*, the following equation can be obtained for the light intensity (I_t):

$$\begin{aligned} I_t &= [\text{oxalate}] \cdot k_2 \cdot [H_2O_2] \cdot Z \\ &= [\text{oxalate}]_0 \cdot e^{(k_1 \cdot [H_2O] + (k_2 + k_3) \cdot [H_2O_2])} \\ &\quad \cdot k_2 \cdot [H_2O_2] \cdot Z \end{aligned} \quad (4)$$

where

$$Z = \frac{k_5 \cdot [F]}{k_4 + k_5 \cdot [F] + k_6 \cdot [Q] + k_7 \cdot [H_2O_2]} \cdot \frac{k_9}{k_8 + k_9} \cdot \frac{k_{11}}{k_{10} + k_{11}} \quad (5)$$

The light emitted from the reaction mixture (L_e, the integrated light intensity) is the portion of the oxalate producing light in the series of reactions

$$L_e = \frac{[\text{oxalate}]_0 \cdot k_2 \cdot [H_2O_2]}{k_1 \cdot [H_2O_2] + (k_2 + k_3) \cdot [H_2O_2]} \cdot Z \quad (6)$$

B. Hydrogen Peroxide Concentration Dependence; Quantitative Relationship for CL Integrated Intensity as a Function of H_2O_2

One of the primary parameters in the PO-CL system is the hydrogen peroxide concentration when the object of the analysis is the determination of the concentration of fluorescent molecules. In the PO-CL reaction, the rate-determining step is the reaction of oxalate with hydrogen peroxide that is equal to the rate of the pseudo first-order light decay. From Equation 3, the rate of oxalate consumption [104,107] is given by:

$$\begin{aligned} f &= k_1 \cdot [H_2O] + (k_2 + k_3) \cdot [H_2O_2] \\ &= A \cdot (B + [H_2O_2]) \end{aligned} \quad (7)$$

where

$$A = k_2 + k_3; \quad B = \frac{k_1 \cdot [H_2O]}{k_2 + k_3} \quad (8)$$

and is shown in Figure 2. A similar relationship can be established for the rise constant

$$r = A' \cdot (B' + [H_2O_2]) \quad (9)$$

as shown in Figure 3 ($A' = 4.42\ 10^{-2}\ s^{-1}\ mol^{-1}$ and $B' = 16.4$ m*M*).

It has been known for some time that the rate of the light decay in organic solvents is

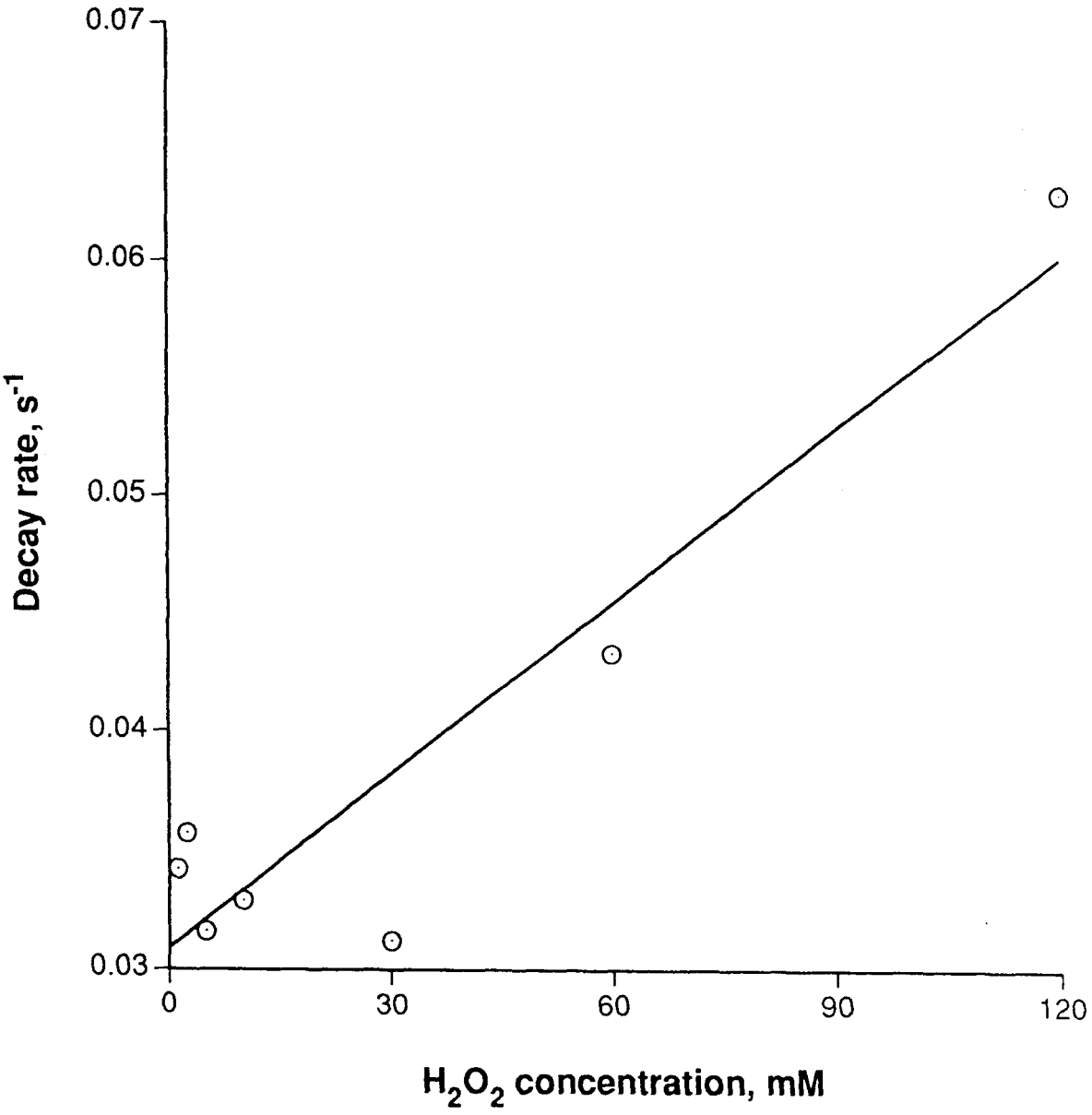

FIGURE 2. The dependence of fall constants on the hydrogen peroxide concentration (data from Reference 104). Conditions: *bis*(2,4,6-trichlorophenyl) oxalate (TCPO) = 0.5 m*M*, 9,10-diphenylanthracene = 0.25 m*M*, imidazole = 2.5 m*M* at pH = 7.0 in 75% aqueous acetonitrile.

primarily determined by the conjugate base of hydrogen peroxide; thus, acidic and basic moderators influence the rate of the reaction substantially. In this respect, the role of additives is to regulate the pH and/or to catalyze the reaction of the hydroperoxide with the oxalate. In Figure 4, the light decay half lives are plotted against the pH. On the basis of this observation, the rate of light decay can be written in the form:

$$f \propto \left(B + [H_2O_2]\right) \cdot [OH^-]^n \qquad (10)$$

where n = 0.3 and [OH^-] is the hydroxide ion concentration. The slope of the curve is –0.3, which indicates the complex protonation equilibrium between the buffer, water, and hydrogen peroxide. Because the moderators influence the rate of the reaction, the "window" in Figure 1 rep-

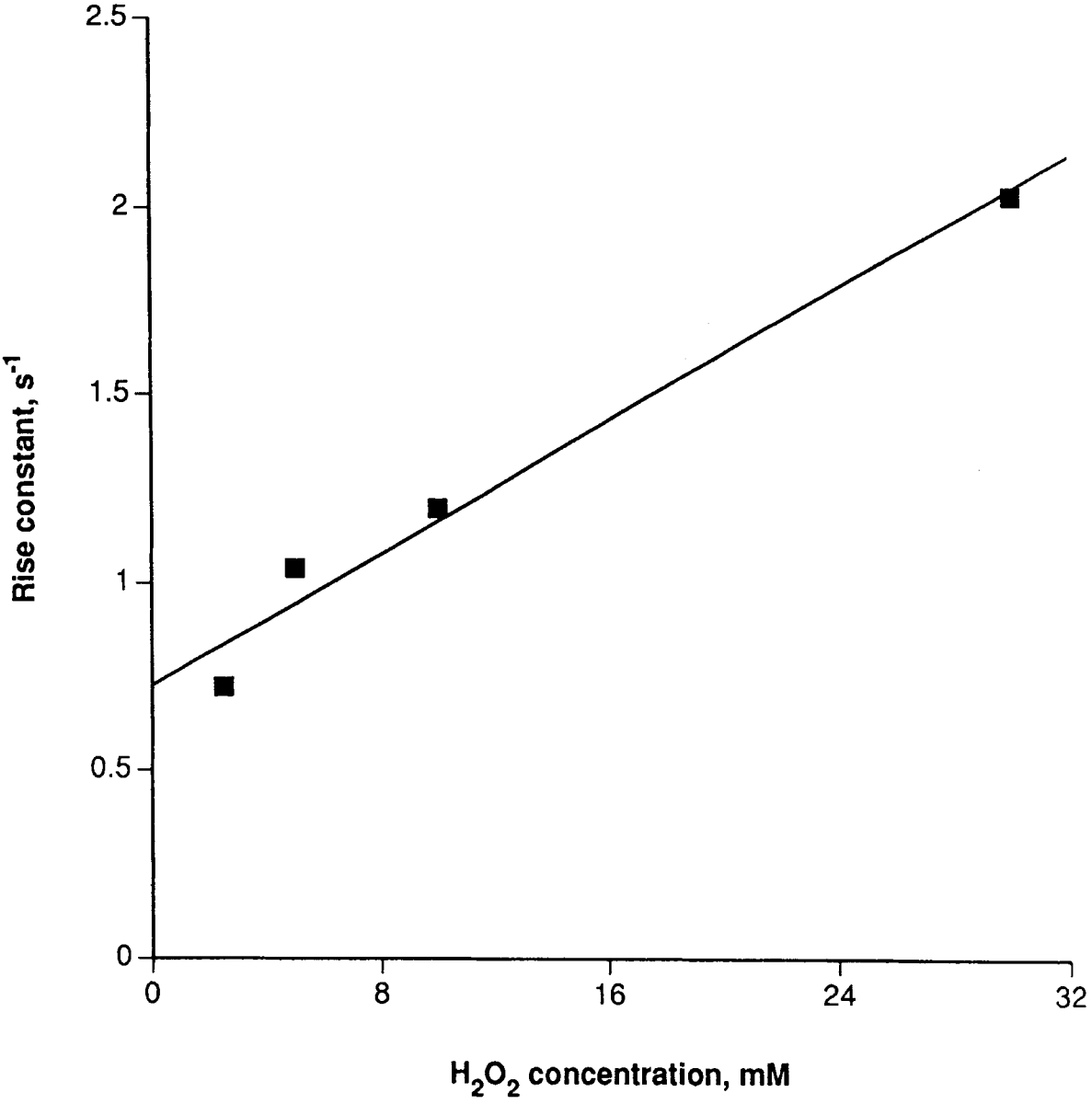

FIGURE 3. The effect of hydrogen peroxide on the rise constant (data from Reference 104). Conditions: *bis*(2,4,6-trichlorophenyl) oxalate (TCPO) = 0.5 m*M*, 9,10-diphenylanthracene = 0.25 m*M*, imidazole = 2.5 m*M* at pH = 7.0 in 75% aqueous acetonitrile.

resents different portions of the chemiluminescent time/intensity profile. In essence, provided that other parameters are not changed, the "optimal" moderator concentration [102,108] is determined where the chemiluminescent light emission profile and efficiency gives the most advantageous response for a given set of conditions.

Equations 4 and 6 can be simplified further by evaluating the effect of fluorophore concentration in Equation 5 and considering that the value of k_5/k_4 is 2–7 $10^3\ M^{-1}$ (depending on the structure of oxalate), a value obtained by several different authors [106,124,125]. The first part of Z in Equation 5 can be rearranged to give the ratio of the two rates, that is:

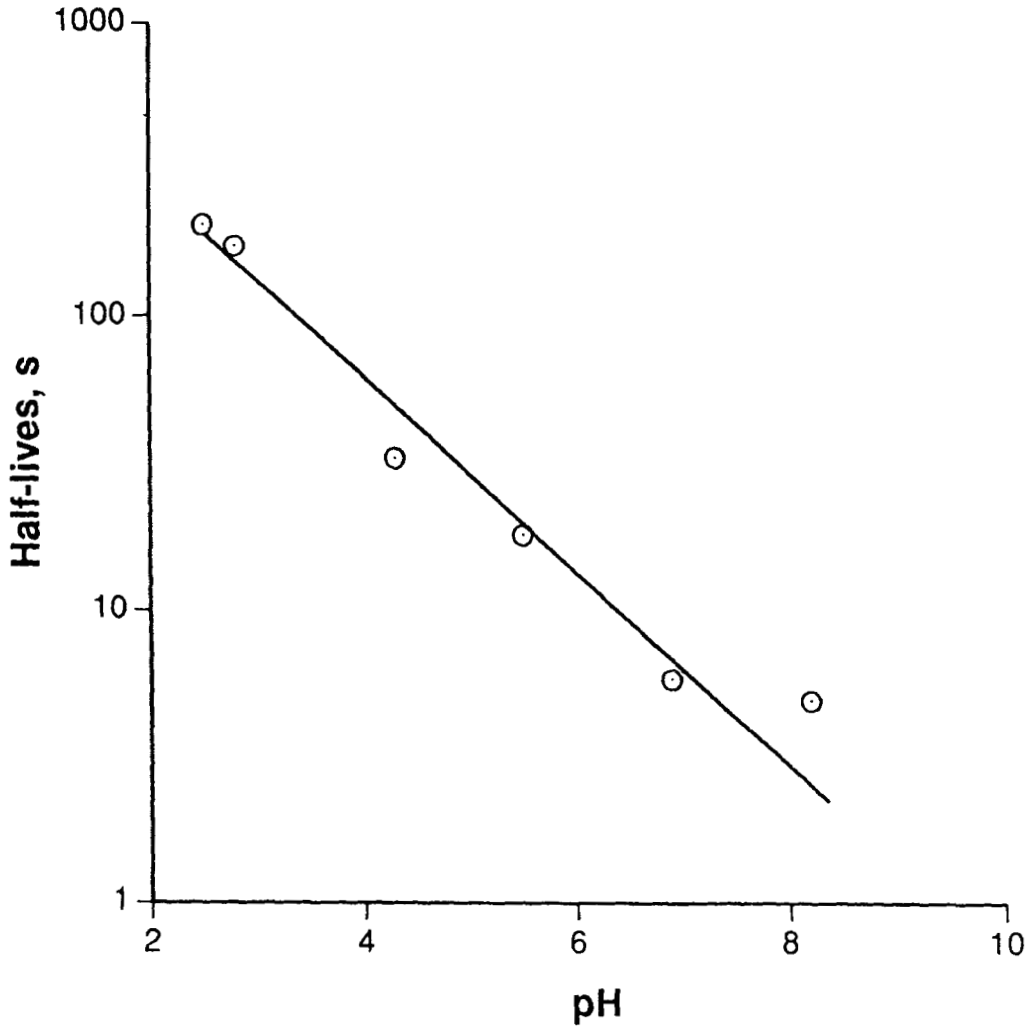

FIGURE 4. The influence of pH on the half-life of the chemiluminescent system (data from Reference 101). Conditions: TCPO = 2.5 m*M*, hydrogen peroxide = 375 m*M*, imidazole = 0.42 m*M* in tetrahydrofuran-ethyl acetate-water mixture.

$$\frac{k_5 \cdot [F]}{k_4 + k_3 \cdot [F] + k_6 \cdot [Q] + k_7 \cdot [H_2O_2]}$$

$$= \frac{\frac{k_5}{k_4} \cdot [F]}{1 + \frac{k_5}{k_4} \cdot [F] + \frac{k_6}{k_4} \cdot [Q] + \frac{k_7}{k_4} \cdot [H_2O_2]} \qquad (11)$$

If the fluorophore concentration is less than 10^{-4} *M*, its effect on the value of the denominator in Equation 11 will be negligible because $k_5 [F]/k_4 < 1$, and the expression varies linearly with the fluorophore concentration, as shown in Equations 12 and 13:

$$I_t = K \cdot [\text{oxalate}]_0 \cdot [H_2O_2] \cdot \frac{[F]}{C + [H_2O_2]} \cdot e^{-A \cdot (B + [H_2O_2]) \cdot t} \qquad (12)$$

$$L_e = K' \cdot \frac{[\text{oxalate}]_0 \cdot [H_2O_2]}{B + [H_2O_2]} \cdot \frac{[F]}{C + [H_2O_2]} \qquad (13)$$

A rough estimate of the maximal light intensity (J) can be obtained from Equation 12 by letting $t = 0$ in I_t.

$$J = K'' \cdot [\text{oxalate}]_0 \cdot [F] \cdot \frac{[H_2O_2]}{C + [H_2O_2]} \quad (14)$$

Orlovic et al. [104] determined light intensity decays, maximal light intensities, and quantum efficiencies at different hydrogen peroxide concentrations for the same series. The data in Figures 2, 5, and 6 were fitted to Equations 7, 13, and 14 (Table 1). The good fit indicates that the model is adequate for modeling these data.

The saturation of the maximal light intensity (J, Equation 14) at high hydrogen peroxide concentrations was observed by several authors [15,31,51,77,102]. At pH 4, however, Orosz found a quasi-linear relationship [107]. This dichotomy can be dissolved by including an additional process (Scheme 1, Pathway 7), which is important at higher pH. The chemiluminescent intermediate, in addition to decomposition by

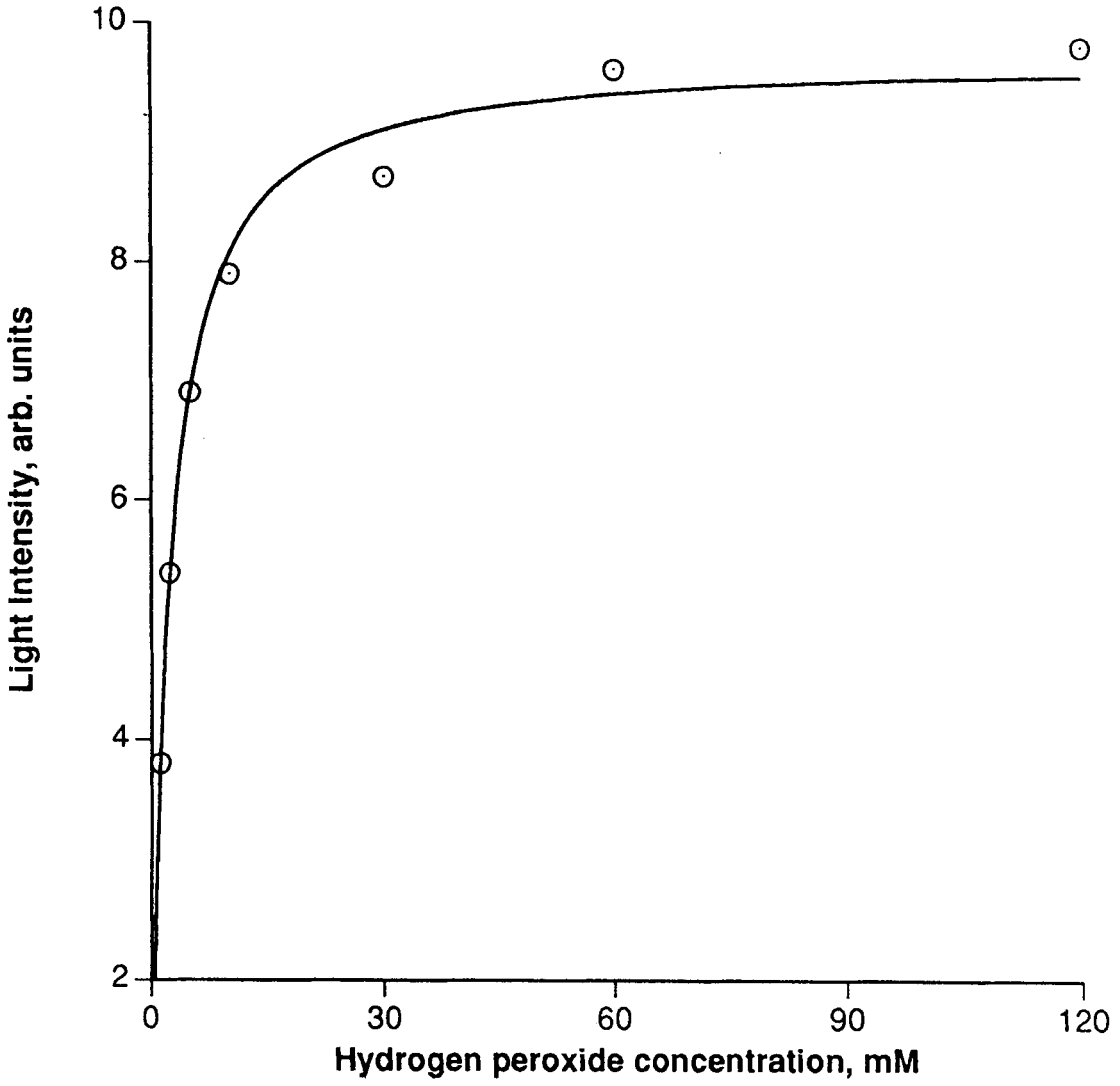

FIGURE 5. Experimental and fitted values (Equation 12, Table 1) on the hydrogen peroxide concentration dependence of the maximal light intensity. Conditions: *bis*(2,4,6-trichlorophenyl) oxalate (TCPO) = 0.5 m*M*, 9,10-diphenylanthracene = 0.25 m*M*, imidazole = 2.5 m*M* at pH = 7.0 in 75% aqueous acetonitrile.

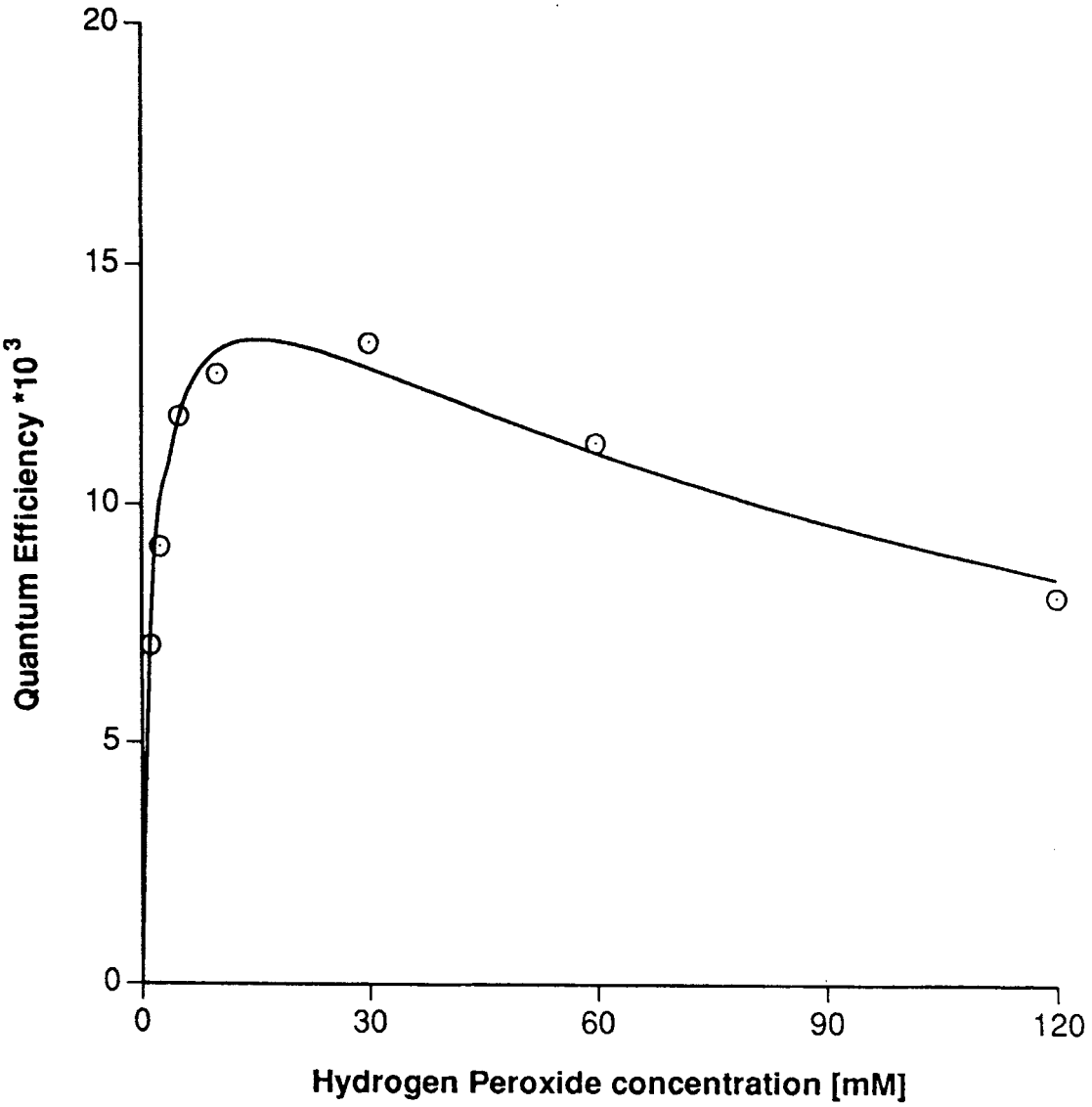

FIGURE 6. The influence of hydrogen peroxide concentration on the quantum efficiency of the PO-CL reaction (data fitted to Equation 11, with the parameters in Table 1). Conditions: *bis*(2,4,6-trichlorophenyl) oxalate (TCPO) = 0.5 m*M*, 9,10-diphenylanthracene = 0.25 m*M*, imidazole = 2.5 m*M* at pH = 7.0 in 75% aqueous acetonitrile.

TABLE 1
Parameters Obtained by Fitting the Data in Figures 2, 5, and 6 for the Parameters in Equations 7, 13, and 14

	Figure 2	Figure 5	Figure 6
B [m*M*]	126.6	—	124.4
C [m*M*]	—	2.04	1.90
R^2	0.886	0.990	0.973

Pathway 4, also reacts with the hydroperoxide anion (Pathway 7).

C. The Effect of Fluorophore and Oxalate Concentration

The rate constant of the pseudo first-order light decay is not influenced by the oxalate concentration, in accordance with the model [104,107]. In the expressions for the light emission, a linear dependence can be seen for the oxalate concentration (Equations 12 through 14), which holds at low pH [107] and at low oxalate concentrations (Figure 7). At higher pH, the dependence deviates from linearity (the slopes are less than 1). Nevertheless, their most important feature is that they increase with increasing oxalate concentration.

When the media are not buffered, and at higher oxalate concentrations, the phenol formed in the reaction lowers the pH, thereby decreasing the rise and fall rates and lower-

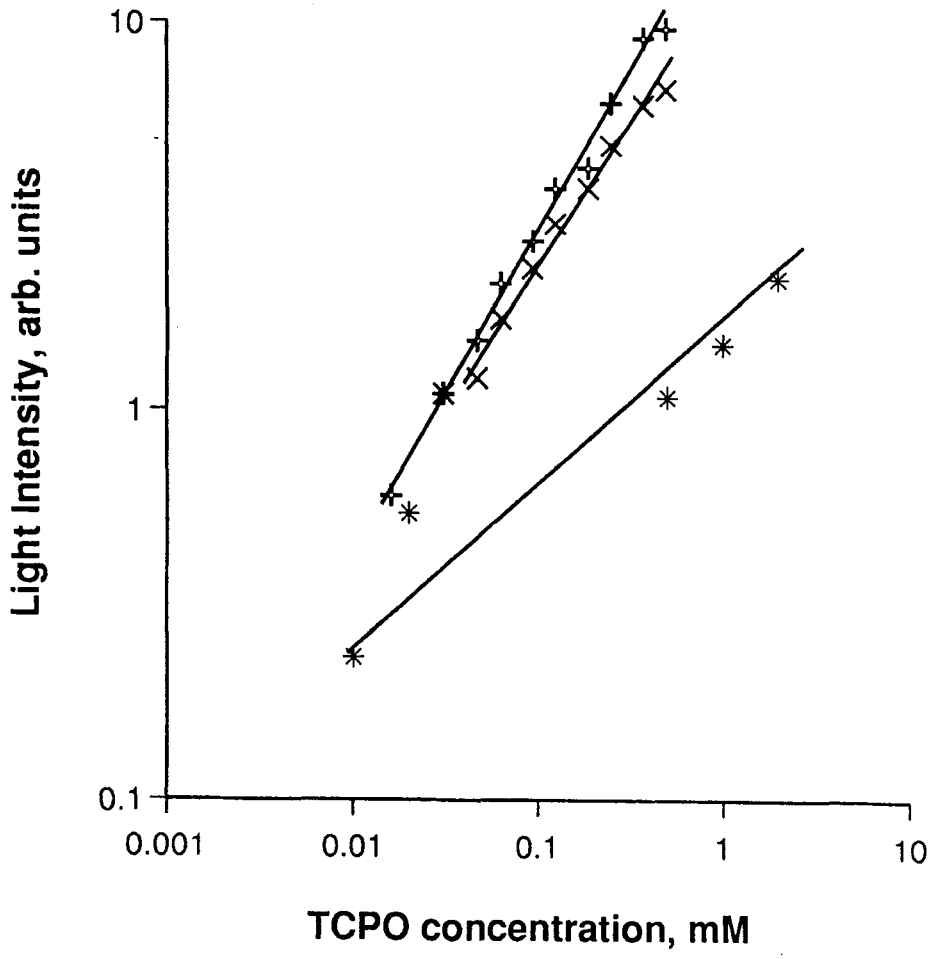

FIGURE 7. Relationship between the light intensities and the oxalate concentration. Data from Reference 104: × 5 m*M*, + –30 m*M* hydrogen peroxide concentration. Conditions: *bis*(2,4,6-trichlorophenyl) oxalate (TCPO) = 0.5 m*M*, 9,10-diphenylanthracene = 0.25 m*M*, imidazole = 2.5 m*M* at pH = 7.0 in 75% aqueous acetonitrile. Data from Reference 102: ✱ –2.5 m*M* hydrogen peroxide concentration; dansyl-alanine (fluorophore) = 0.025 m*M*, imidazole = 1 m*M* at pH = 7 in 80% aqueous acetonitrile.

ing the maximal light intensity [103,126]. Quenching by the phenol and the reabsorption of the emitted light especially by nitrophenolate anion may also contribute to the decrease in light intensity.

In the reaction catalyzed by imidazole, the quantum yield increased with increasing oxalate concentration [104]. This latter observation indicates that the model is an approximation only and that the catalyst can play a significant and complex role in the reaction, altering the mechanism of the light production [51,115].

The rate of light decay is not dependent on the concentration of fluorophore [104, 106,107], as indicated in the model (Equation 7). The maximal light intensity (Equation 14) changed linearly with the fluorophore concentration through several orders of magnitude [9,92,107]. A similar relationship was established for the quantum yields [104] (Equation 13).

IV. COUPLING THE MODEL AND THE PO-CL DETECTION

A. Detector Parameters

It is generally observed that increasing detector volume increases the chemiluminescent signal obtained [83,84,101,108]. The effect of increasing detector volume on chromatographic performance has been studied extensively [83,101]. From these studies, the following conclusions may be reached:

1. Increasing the detector volume by dilution of the reagent flow(s) should not affect the chromatographic separation.

2. The volume of the detector cell should be no larger than the elution volume of the narrowest peak of interest. As a practical guide, the cell volume should be smaller than the peak "volume" multiplied by the dilution caused by the added reagents.

3. The differential model detector signal increases with increasing cell volume as it approaches the "integrating" detector model. In practice, however, this is not always true, as demonstrated [83] in Figure 8. The chemiluminescent signal approaches a maximum when the detector cell is 0.2 to 0.3 of the peak width at half height ($w_{1/2}$). Hanaoka's studies [108] showed that for broad peaks, a cell volume greater than 100 µl, the signal does not increase significantly.

Another factor influencing the detection parameters is the configuration of the light collection apparatus. deJong and his co-workers [83,101] prepared an "integrating" detector by employing *bis*(2,4-dinitrophenyl) oxalate (DNPO) activator and large detector cell volume. With less activated oxalates, that is, *bis*(2,4,6-trichlorophenyl) oxalate (TCPO), in the pH range of 7 to 8, the half-life of the reaction ranged from 5 to 20 s.

In typical experimental setups, the detector volume rarely exceeds 100 µl, the combined eluent and reagent flows are generally larger than 2 cm^3 per min. Under these conditions, the residence time of the reaction mixture in the detector is approximately 3 s or less, and thus the detector can be treated as differential detector and its response can be approximated by Equation 12 for the light intensity.

B. Delay After Mixing the Reagents

The differential detector is very sensitive to the position of the window along the chemiluminescent time/intensity profile (Figure 1). Before reaching the maximum, the time/intensity profile indicates that there is a very sensitive response to even small changes in flow, making it difficult to achieve good stability for analytical purposes. The best position for the detector on the time/intensity curve is at or slightly later than the

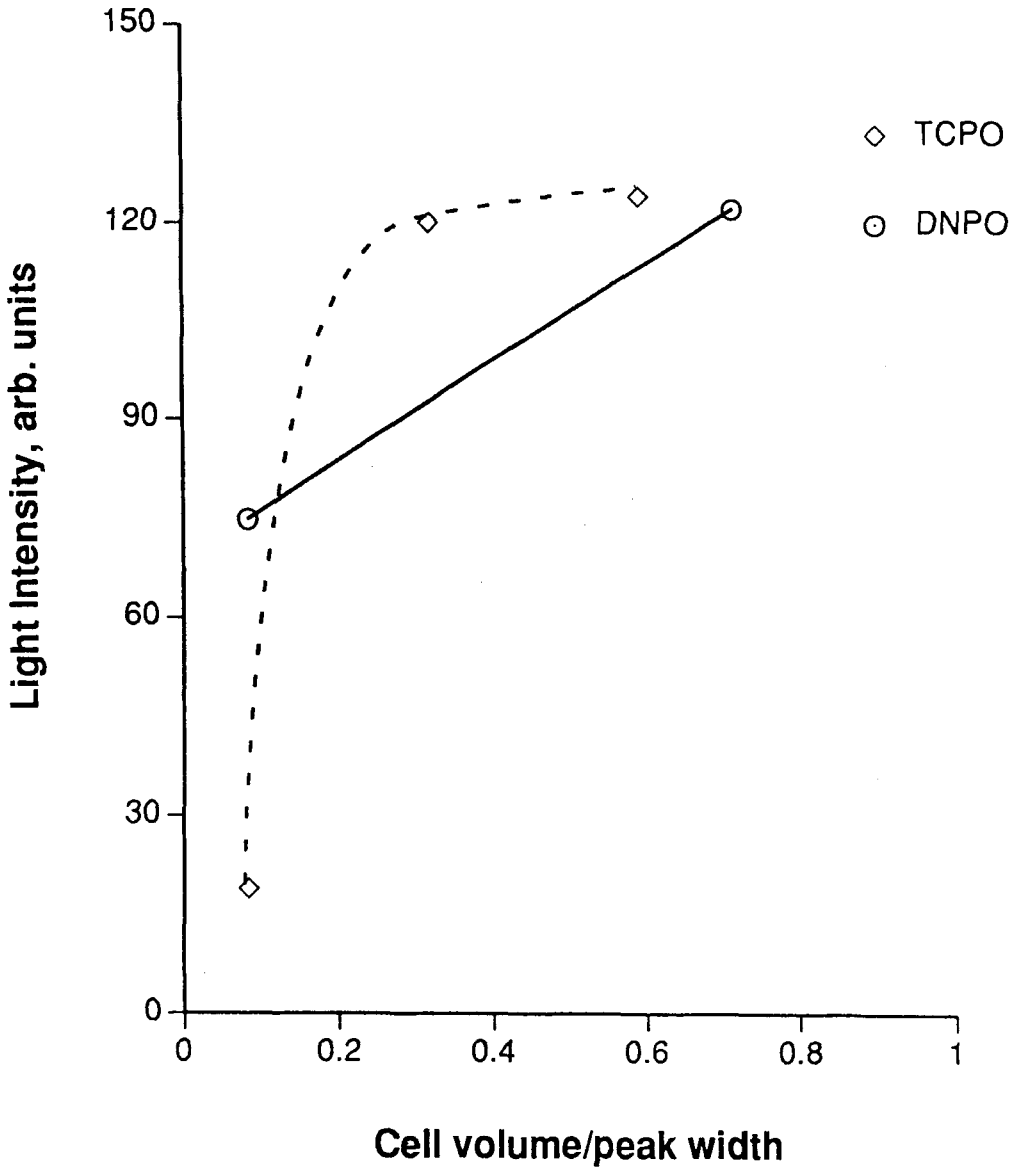

FIGURE 8. The influence of the ratio of detector volume and the peak width on the chemiluminescent signal (data taken from Reference 83). DNPO = *bis*(2,4-dinitrophenyl) oxalate.

maximum. Changing the eluent or reagent flows and thereby adjusting the concentration of the reagents, changes the delay time and, consequently the position of the window.

The effect of fluorophore and oxalate concentrations on the light intensity (Equation 12) and thus on the detector response is straightforward: the rate constants for the double-exponential curve (Figure 1) do not change with the change in concentrations of these two reagents. The fluorophore causes a linear increase in light emission with concentration, as does an increase in oxalate concentration.

In Figure 9, the effect of hydrogen peroxide concentration on the light intensity is shown at different delay times using the parameters determined earlier from Reference 104 in Equation 1 (Table 1). The maximum light intensity reaches saturation with increasing hydrogen peroxide concentration

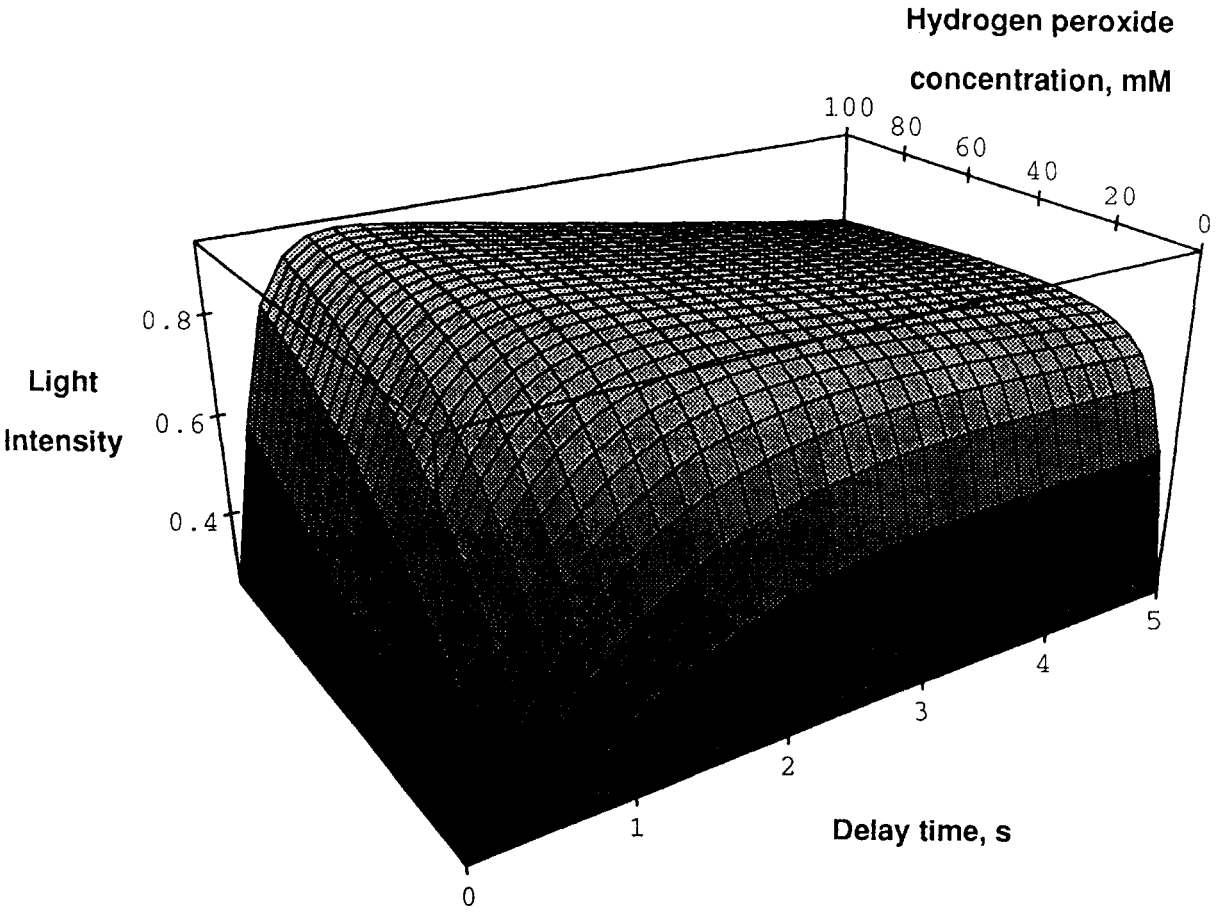

FIGURE 9. Simulation of the effect of hydrogen peroxide concentration and the delay time on the detector response using Equation 1 and the parameters obtained from Figures 2 and 3.

(Equation 14) up to 1 s delay time (Figure 9). Simultaneously, the time required to reach maximum becomes shorter. At shorter delays, however, increasing the hydrogen peroxide concentration gives a light intensity curve that asymptotically approaches the maximum value. This means that — depending on the dead volume of the system — monotonous increase, or "optimal" hydrogen peroxide concentration can be observed by increasing the hydrogen peroxide concentration! The response at this "optimal" concentration (e.g., at 5 s delay time), however, may be much less than the response at shorter (e.g., at 1 s) delay times.

In a flow system, the eluate and reactant concentrations ($[F]_0$-fluorophore, $[oxalate]_0$-oxalate, and $[H_2O_2]_0$-hydrogen peroxide concentrations of the reagent solutions) are diluted by the eluent and the other reagent flows (Y_{col}-eluent, Y_{ox}-oxalate, Y_{H2O2}-hydrogen peroxide flow rate), that is,

$$[F] = [F]_0 \cdot \frac{Y_{col}}{Y_{col} + Y_{ox} + Y_{H_2O_2}} \qquad (15)$$

$$[oxalate] = [oxalate]_0 \cdot \frac{Y_{col}}{Y_{col} + Y_{ox} + Y_{H_2O_2}} \qquad (16)$$

$$[H_2O_2] = [H_2O_2]_0 \cdot \frac{Y_{col}}{Y_{col} + Y_{ox} + Y_{H_2O_2}} \qquad (17)$$

The delay time (t_d) is determined by V_0, the dead volume between the mixing point and the detector, and the combined reagent and eluent flows:

$$t_d = \frac{V_0}{Y_{col} + Y_{ox} + Y_{H_2O_2}} \qquad (18)$$

Combining Equations 1 and 12, the expression for the light intensity inside the cell can be obtained in the form of

$$I_{t_d} = K''' \cdot \frac{[F]_0 \cdot [oxalate]_0 \cdot [H_2O_2]}{C + [H_2O_2]_0 \cdot \dfrac{Y_{H_2O_2}}{Y_{col} + Y_{ox} + Y_{H_2O_2}}} \cdot \frac{Y_{col} + Y_{ox} + Y_{H_2O_2}}{\left(Y_{col} + Y_{ox} + Y_{H_2O_2}\right)^3} \cdot \left(e^{-f \cdot t_d} - e^{-r \cdot t_d}\right) \qquad (19)$$

where the parameters f, r, and t_d are determined by Equations 7, 9, and 18.

On the basis of this expression, qualitatively the same behavior is expected upon changing the oxalate and eluent flows if the fluorescent peak width is much larger than the detector volume. The effect of dead volume and flow rate at two different hydrogen peroxide concentrations is shown in Figures 10 and 11. Optimum flow rates can be established for each dead volume. It should be pointed out that at different dead volumes, the optimal eluent flows are not equal

The hydrogen peroxide concentration has a more complex relationship with chemiluminescent intensity. This property, however, does not yield a substantially different response from Figures 12 and 13. The change of kinetics at higher hydrogen peroxide concentrations (Figure 13) can be deduced from a shift of the optimal delay: If the time to reach the maximal light intensity is the same, the optimal dead volume shifts toward the larger volumes. In contrast, in Figure 13, the increasing hydrogen peroxide flow rate shifts the maximal light intensity toward the smaller dead volumes (compare with Figure 10).

C. The Optimization Process

After the static experiments, where the starting points of the flow system optimization were determined, the optimization of the flow system is generally accomplished by changing the reagent flows and concentrations in a system with a certain dead volume.

Typical responses were calculated (Equation 19) for two dead volumes: With 5 µl delay, the reaction is in the rise phase (Figure 14), whereas with 200 µl dead volume at 3 cm^3 per min combined flow rate positions the window beyond the maximum light emission (Figure 15). Both the oxalate and the hydrogen peroxide flow rates (Figures 14 and 15) have optimal values, yielding a response surface with one maximum. Depending on the flow rate values and the reagent concentrations, at certain points on the surface, the chemiluminescent signal can be observed to increase by increasing any of the reagent flow rates or by increasing only one reagent flow rate. Similarly, in certain points, it can decrease by increasing both or only one flow rate. Identifying the gradient of the direction for the optimal response is often possible. The optimization process, however, may need several interactions to attain the maximum on the surface. Furthermore, one may not wish to work at the maximum when it is "unstable" to small changes in any one of the parameters (e.g., Figure 14), but should rather select a point on the surface as in Figure 15, where the change in instrumental parameters will generate only small changes in the light intensity (e.g., hydrogen peroxide = 2.0, oxalate = 0.8 cm^3 per min). With this approach, it is possible to understand how an increase in chemiluminescent

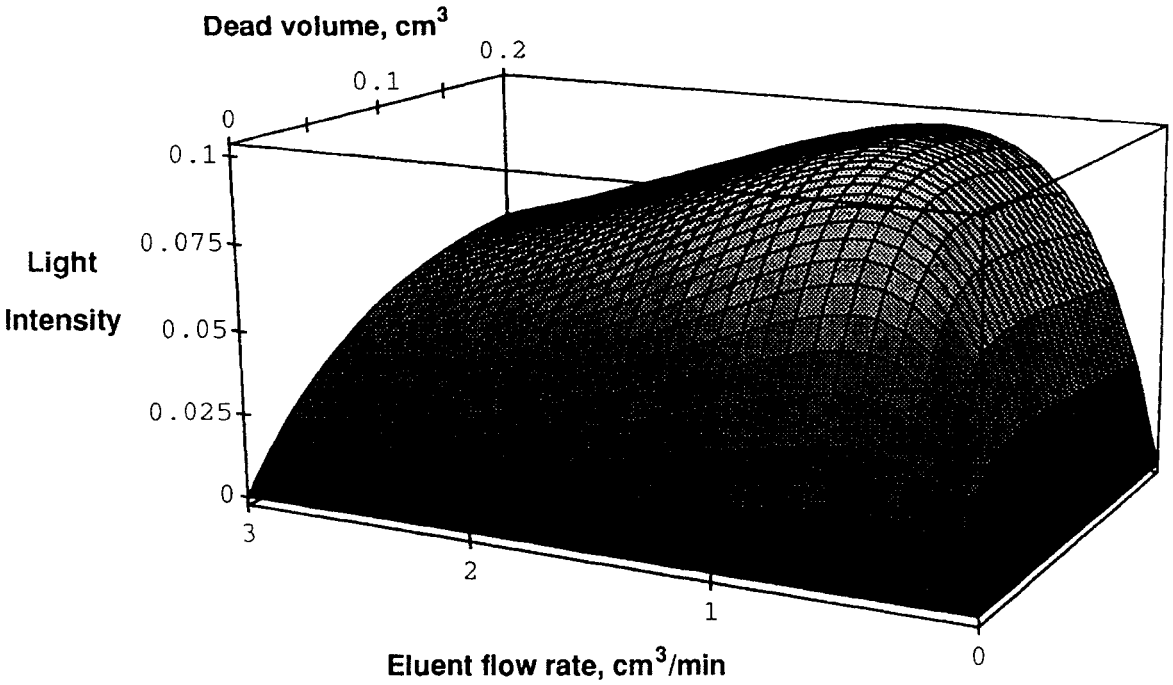

FIGURE 10. Simulation of the effect of eluent flow rate on the detector response based on Equation 19. Flow rates: TCPO = 1 cm^3 per min; hydrogen peroxide = 30 m*M*, 1 cm^3 per min.

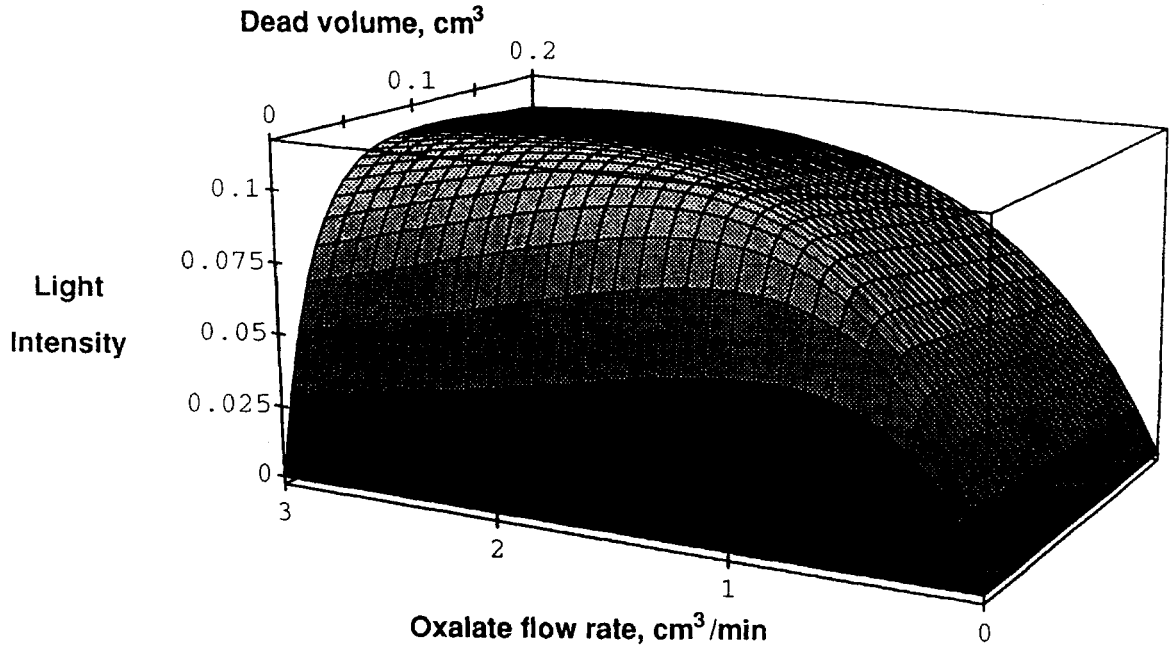

FIGURE 11. The effect of dead volume and the oxalate flow rate on the chemiluminescent detector response (Equation 19). Flow rates: eluent = 1 cm^3 per min; hydrogen peroxide = 300 m*M*, 1 cm^3 per min.

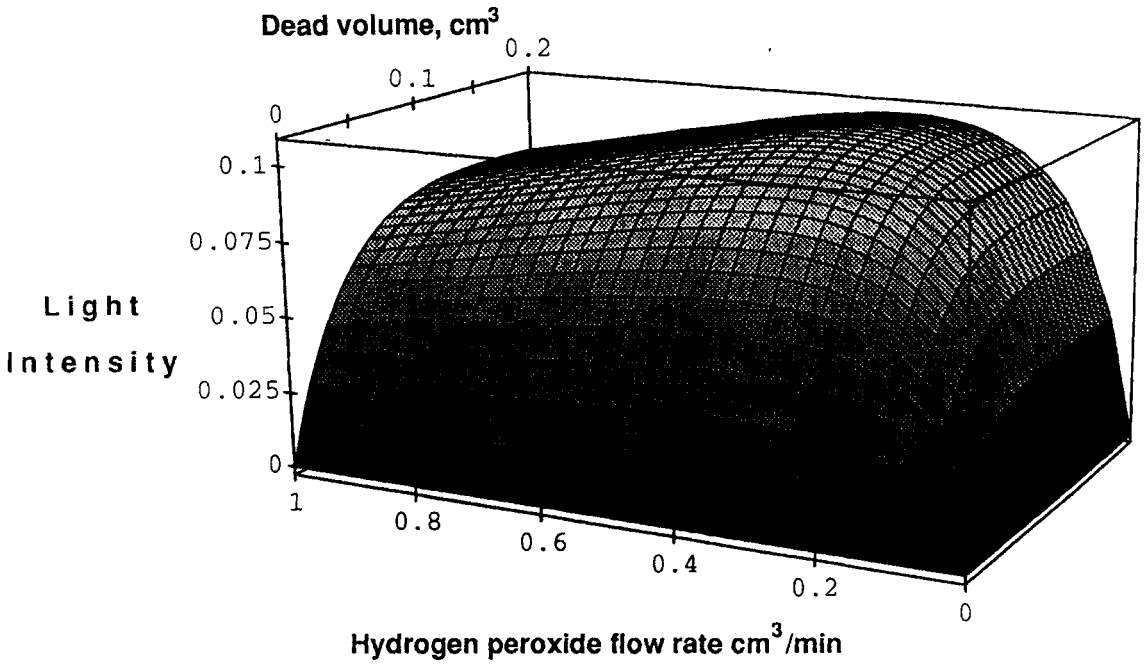

FIGURE 12. The effect of low concentration of hydrogen peroxide (30 m*M*) and the dead volume on the detector response (Equation 19). The oxalate and eluent flows are 1 cm^3 per min.

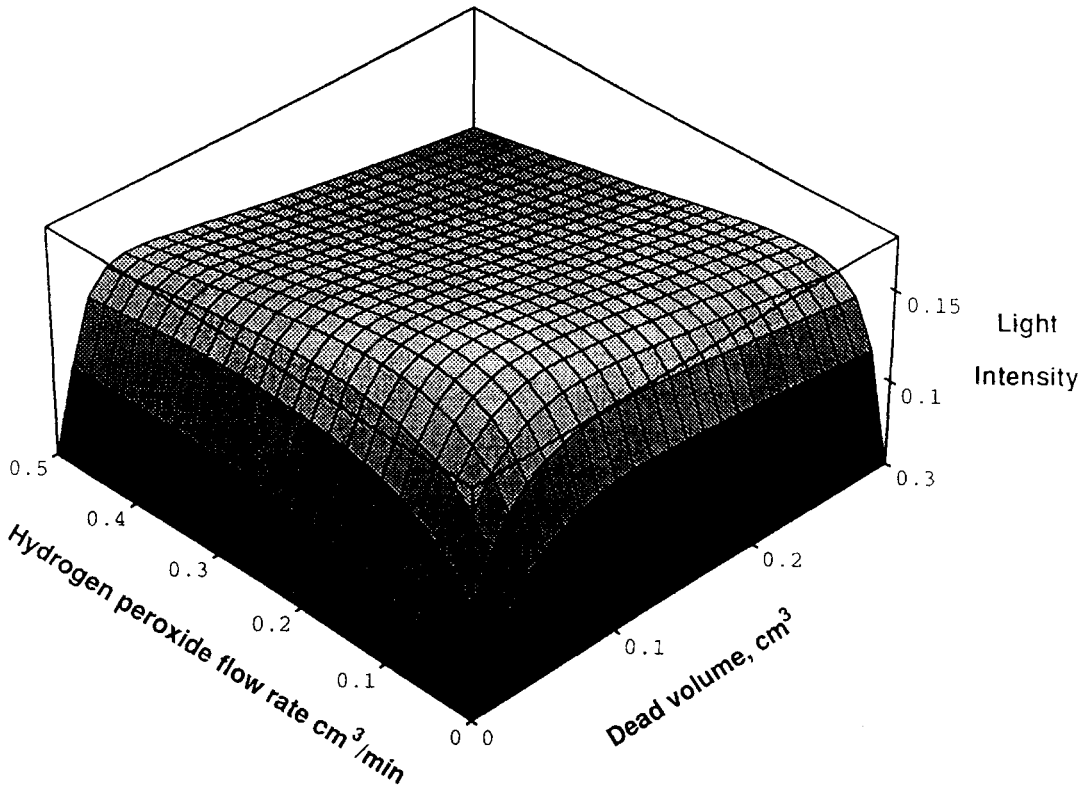

FIGURE 13. Simulated relationship between the dead volume, the hydrogen peroxide flow rate (300 m*M*), and the chemiluminescent response (Equation 19). The oxalate and eluent flow rates are 1 cm^3 per min.

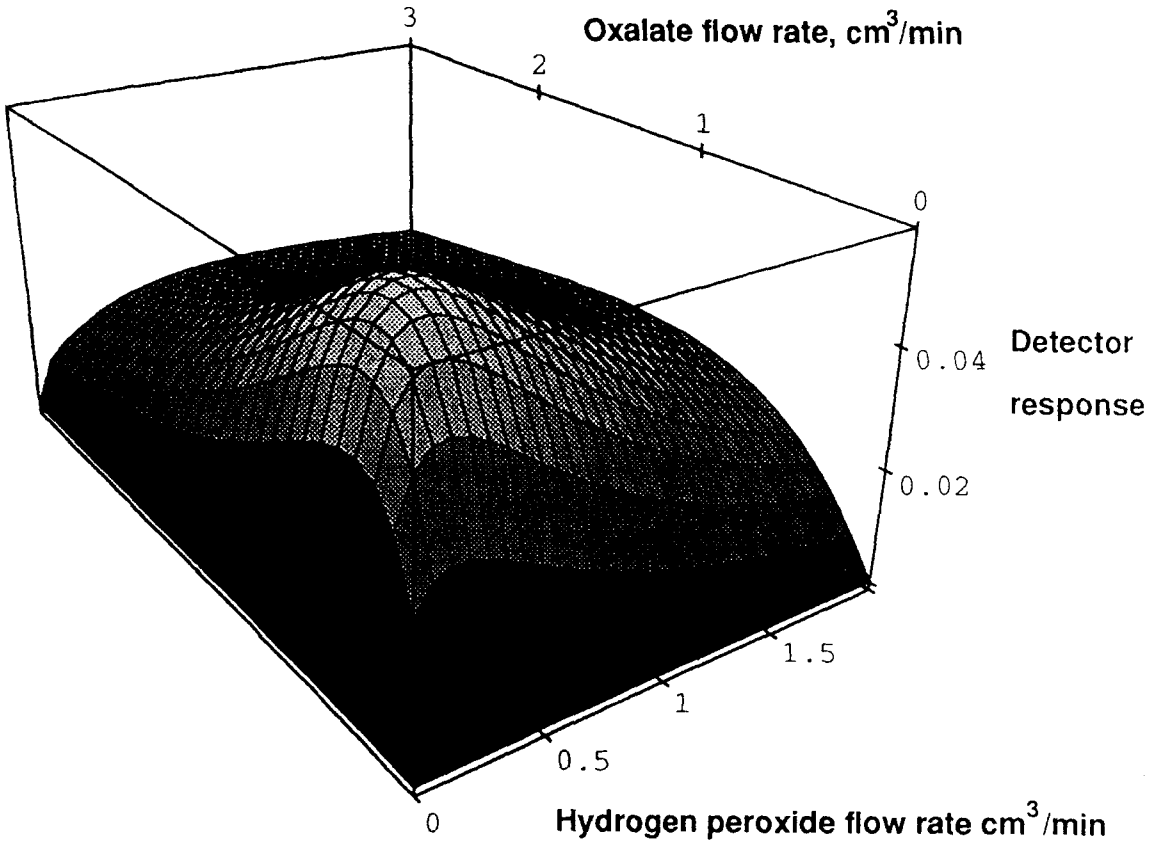

FIGURE 14. The change of chemiluminescent response (Equation 19) by changing oxalate and hydrogen peroxide (300 m*M*) flow rates at 5 µl dead volume and 1 cm^3 per min eluent flow rate.

response can occur when decreasing the hydrogen peroxide flow rate, while at the same time increasing oxalate flow rate [7].

Changing the reagent concentrations introduces other parameters, but these effects can be interpreted by using the correlations given in Figures 9 through 13 (e.g., having the oxalate and hydrogen peroxide flow rates at certain values or depending on the delay in the system) (Figures 14 and 15). By changing the hydrogen peroxide concentration, one observes a linear increase in the detector response (Figure 9; delay is less than 1 s) or a curve showing "maximal" detector response (Figure 9; delay time is greater than 3 s) [7,100].

The parameters used in this analysis may not be appropriate for all of the varieties of CL detector available, but the mechanism and the kinetic derivation should be applicable to other systems. Keeping this in mind, the response surfaces that are created indicate the actual position for the CL reaction (at least qualitatively), thereby aiding application chemists in visualizing the results and allowing them to predict the influence of any modification in instrumental parameters on the detector response.

VI. QUENCHED PEROXYOXALATE CHEMILUMINESCENCE

The quenched peroxyoxalate chemiluminescence was first observed by Honda et

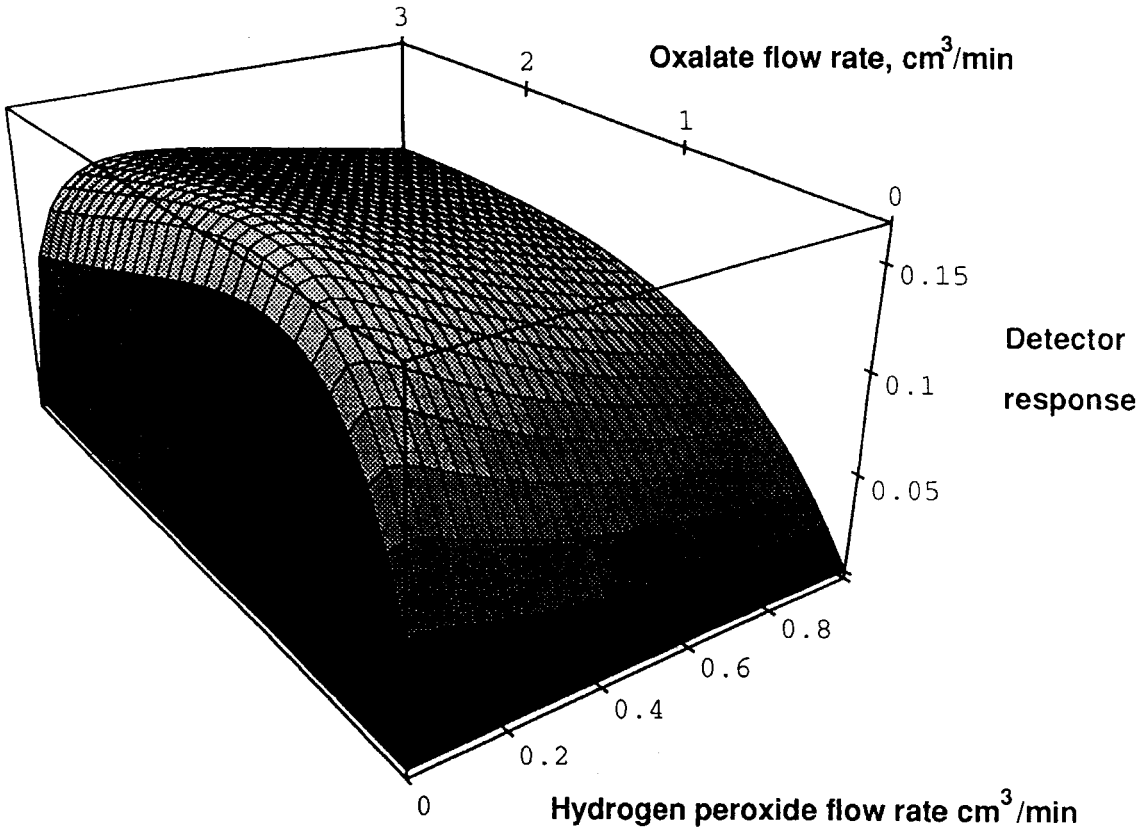

FIGURE 15. The influence of oxalate and hydrogen peroxide (300 m*M*) flow rates on the detector response at 200 µl dead volume. The eluent flow is 1 cm^3 per min.

al. [40], later studied in detail by van Zoonen [43,71], Gooijer [72,73] and Grayeski [74], and further discussed on the theoretical basis by Gooijer and Velthorst [72,73]. Here, we attempt to show that the identical mechanism above can be employed to quantitatively explain some characteristic of the quenched process using the parameters determined in static experiments.

The observation that the light intensity decreases when certain quenchers are present (e.g., halides [40], amines, or sulfur-containing compounds [71]) has been exploited for analytical purposes. (It should be mentioned that quenching with nitrogen-containing compounds having less or more basic properties is not unequivocal: these compounds can act not only as quenchers, but also as accelerators for a chemiluminescent reaction. This acceleration — because the detectors are mostly differential — can also act as a formal quenching, decreasing the signal as it was demonstrated by DeVasto and Grayeski [74].)

A Stern-Volmer relationship between the quencher concentration and the light intensity can be expressed as

$$\frac{I_0}{I_Q} = 1 + k_Q \cdot [Q] \qquad (20)$$

where I_0 is the light intensity in the absence, I_Q is the presence of the quencher, k_Q is the quenching constant characteristic of the quencher, and [Q] is its concentration [72]. From the expression derived for either the

differential or the integrating detector (Equations 4 through 6), the ratio of the light intensity as a function of [Q] leads to the expression:

$$\frac{I_0}{I_Q} = 1 + \frac{k_6}{k_4 + k_5 \cdot [F] + k_7 \cdot [H_2O_2]} \cdot [Q]$$

$$= 1 + \frac{\frac{k_6}{k_4}}{1 + \frac{k_5}{k_4} \cdot [F] + \frac{k_7}{k_4} \cdot [H_2O_2]} \cdot [Q] \qquad (21)$$

It was noted earlier [106,124,125] (Equation 11) that the value of k_5/k_4 is in the range of 2 to 7 10^3 M^{-1}. In quenching experiments, the concentration of fluorophore used [72,73] is less than 10^{-4} M; thus, k_5 $[F]/k_4$ is negligible. The ratio of k_4/k_7 in the denominator expresses the sensitivity of the chemiluminescent intermediate toward the attack of hydrogen peroxide. Its value (Table 1, C) is about 2 mM at pH = 7 in imidazole buffer. Below this concentration, the hydrogen peroxide does not influence the value of the denominator significantly.

Thus, the ratio of k_6/k_4 determines the value of k_Q. Furthermore, if the mechanism for quenching is also by electron transfer, it is reasonable to anticipate that effective quenchers will have lower oxidation potentials than the fluorophores and thus, k_6/k_4 should be greater than k_5/k_4. For different fluorophores, values between 2.6 to 4.4 10^4 M^{-1} were obtained for the quenching constant of 2-mercapto-1-methylimidazole by van Zoonen and his co-workers [71], which is in accord with an electron transfer quenching mechanism [105].

No significant differences between TCPO and DNPO have been reported for the excitation of different fluorophores [127,128]. Therefore, the value of k_5 is thought to be independent of the nature of the oxalate, but dependent on the fluorophore.

A similar insensitivity to oxalate structures is expected for the quencher as well (i.e., the value of k_6 is expected to be the same for a specific quencher):

$$k_Q = \frac{K''''}{k_4} \qquad (22)$$

where K'''' is the experimental parameter determined by the nature of the quencher, the conditions, solvent, etc., but not by the nature of the oxalate. The chemiluminescent intermediates generated from more electronegatively substituted aryl oxalates are expected to decompose faster. In other words, k_4 is larger for DNPO than for TCPO; thus, the quenching constant for DNPO is smaller than for TCPO.

An interesting result is that in contrast to the expectation that the quenching constant would be higher at low fluorescer concentrations, the effect of fluorophore concentration can be ignored below a certain concentration (Figure 16). This implies that less sensitive photodetectors may be applied in this analytical method.

In summary, it has been shown that even in this simple mechanistic treatment, the quenching constant is

1. independent of the oxalate and the hydrogen peroxide concentration up to 10^{-3} M;
2. independent of the nature and the concentration of the fluorophore up to 10^{-4} M; and
3. dependent on the nature of oxalate in agreement with the observations of Gooijer et al. [72,73].

An alternative approach in the derivation of these relationships for the quenching constant is derived from the assumption that the quencher reacts with the encounter complex (XF) [72].

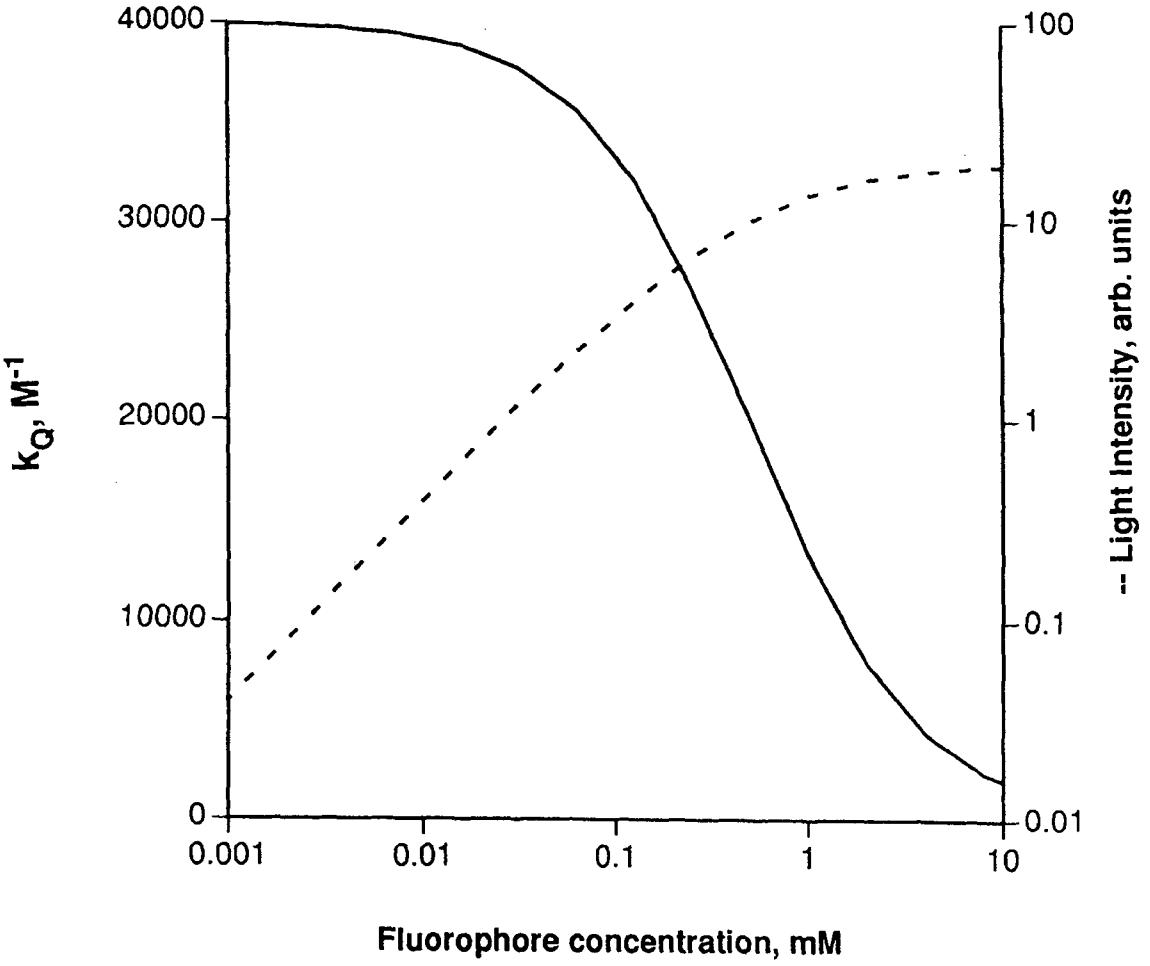

FIGURE 16. Simulated graph showing the apparent value of k_Q (continuous line) and the light intensity (dashed line) by varying the fluorophore concentration (Equation 21). Simulation parameters: $k_6/k_4 = 4.0\ 10^4\ M^{-1}$; $k_5/k_4 = 2.0\ 10^3\ M^{-1}$.

REFERENCES

1. Curtis, T. G.; Seitz, W. R. *J. Chromatography,* **1977,** *134,* 513–516.
2. Curtis, T. G.; Seitz, W. R. *J. Chromatography,* **1977,** *134,* 343–350.
3. Weber, A. J.; Grayesky, M. L. *Anal. Chem.* **1987,** *59(10),* 1452–1457.
4. Wu, N.; Huie, C. *J. Chromatography,* **1993,** *634(2),* 309–315.
5. Sandmann, B.; Grayeski, M. *Chromatographia,* **1994,** *38(3-4),* 163–167.
6. Kwakman, P. J. M.; Brinkman, U. A. T. *Anal. Chim. Acta.* **1992,** *266,* 175–192.
7. Baeyens, W.; Bruggeman, J.; Dewaele, C.; Lin, B.; Imai, K. *J. Biolum. Chemilum.* **1990,** *5,* 13–23.
8. Givens, R. S.; Jencen, D. A.; Riley, C. M.; Stobaugh, J. F.; Chokshi, H.; Hanaoka, N. *J. Pharm. Biomed. Anal.* **1990,** *8(6),* 477–491.
9. Imai, K., Chemiluminescence detection system for high-performance liquid chromatography, in *Bioluminescence and Chemiluminescence,* Part B, M. A. DeLuca, W. D. McElroy, Eds.; Academic Press: New York, 1986; pp 435–449.
10. Imai, K.; Nishitani, A.; Tsukamoto, Y. *Chromatographia,* **1987,** *24,* 77–81.

11. Imai, K.; Nishitani, A.; Akitomo, H.; Tsukamoto, Y. *J. Biolum. Chemilum.* **1989,** *4,* 500–504.

12. Yan, B.; Lewis, S. W.; Worsfold, P. J.; Lancaster, J. S.; Gachanja, A. *Anal. Chim. Acta.* **1991,** *150,* 145–155.

13. Nondek, L.; Milofsky, R. E.; Birks, J. W. *Chromatographia,* **1991,** *32(1/2),* 33–39.

14. Yoshida, S.; Urakami, K.; Kito, M.; Takeshima, S.; Hirose, S. *J. Chromatography,* **1990,** *530,* 57–64.

15. Cepas, J.; Silva, M.; Perezbendito, D. *Anal. Chem.* **1994,** *66(22),* 4079–4084.

16. Hayakawa, K.; Imaizumi, N.; Miyazaki, *M. Biomed. Chrom.* **1991,** *5(4),* 148–52.

17. Hayakawa, K.; Butoh, M.; Miyazaki, M. *Anal. Chim. Acta.* **1992,** *266,* 251–256.

18. Hayakawa, K.; Minogawa, E.; Yokoyama, T.; Miyazaki, M.; Imai, K. *Biomed. Chrom.* **1992,** *6(2),* 84–7.

19. Mann, B.; Grayeski, M. L. *Biomed. Chrom.* **1991,** *5(1),* 47–52.

20. Nakashima, K.; Suetsugu, K.; Yoshida, K.; Akiyama, S.; Uzu, S.; Imai, K. *Biomed. Chrom.* **1992,** *6(3),* 149–54.

21. Nakashima, K.; Nagata, M.; Takahashi, M.; Akiyama, S. *Biomed. Chrom.* **1992,** *6(2),* 55–8.

22. Sugiura, M.; Kanda, S.; Imai, K. *Biomed. Chrom.* **1993,** *7(3),* 149–54.

23. Lewis, S. W.; Worsfold, P. J.; Lynes, A.; McKerrell, E. H. *Anal. Chim. Acta.* **1992,** *266,* 257–264.

24. Kwakman, P. J. M.; Brinkman, U. A. T.; Frei, R. W.; de Jong, G. J. *Chromatographia,* **1987,** *24,* 395–399.

25. Kwakman, P. J. M.; Kamminga, D. A.; Brinkman, U. A. T. *J. Chrom.* **1991,** *553,* 345–356.

26. Uzu, S.; Imai, K.; Nakashima, K.; Akiyama, S. *Analyst,* **1991,** *116(12),* 1353–7.

27. Uzu, S.; Imai, K.; Nakashima, K.; Akiyama, S. *Biomed. Chrom.* **1991,** *5(4),* 184–5.

28. Uzu, S.; Imai, K.; Nakashima, K.; Akiyama, S. *J. Pharm. Biomed. Anal.* **1992,** *10(10-12),* 979–984.

29. Toyooka, T.; Ishibashi, M.; Terao, T. *J. Chromatography,* **1992,** *627(1-2),* 75–86.

30. Toyooka, T.; Chokshi, H. P.; Givens, R. S.; Carlson, R. G.; Lunte, S. M.; Kuwana, T. *Biomed. Chrom.* **1993,** *7(4),* 208–16.

31. Fu, C.; Xu, H.; Wang, Z. *J. Chromatography,* **1993,** *634(2),* 221–227.

32. Gachanja, A.; Lewis, S.; Worsfold, P. *J. Chrom. A.* **1995,** *704(2),* 329–337.

33. Higashidate, S.; Imai, K. *Analyst,* **1992,** *117(12),* 1863–8.

34. Higashidate, S.; Imai, K.; Prados, P.; Adachiakahane, S.; Nagao, T. *Biomed. Chrom.* **1994,** *8(1),* 19–21.

35. Imai, K.; Higashidate, S.; PR Prados, T. S.; Adachiakahane, S.; Nagao, T. *Biol. Pharm. Bull.* **1994,** *17(7),* 907–910.

36. Lewis, S.; Worsfold, P.; Mckerrell, E. *J. Chrom. A.* **1994,** *667(1-2),* 91–98.

37. Prados, P.; Higashidate, S.; Imai, K.; Sato, Y.; Nagao, T. *Biomed. Chrom.* **1994,** *8(1),* 49–51.

38. Prados, P.; Higashidate, S.; Imai, K. *Biomed. Chrom.* **1994,** *8(1),* 1–8.

39. Sandmann, B.; Grayeski, M. *J. Chrom. B Biomed. Appl.* **1994,** *653(2),* 123–130.

40. Honda, K.; Imai, K. *Anal. Chem.* **1983,** *55(6),* 940–943.

41. Mahant, V. K.; Miller, J. N.; Thakrar, H. *Anal. Chim. Acta.* **1983,** *145,* 203–206.

42. Zoonen, P. V.; Kamminga, D. A.; Gooijer, C.; Velthorst, N. H.; Frei, R. W. *Anal. Chim. Acta.* **1985,** *167,* 249–256.

43. Zoonen, P. V.; Kamminga, D. A.; Gooijer, C.; Velthorst, N. H.; Frei, R. W. *Anal. Chem.* **1986,** *58(6),* 1245–1248.

44. Katayama, M.; Takeuchi, H.; Taniguchi, H. *Anal. Lett.* **1991,** *24(6),* 1005–1015.

45. DeFillipo, K. A.; Grayeski, M. L. *Anal. Chim. Acta.* **1991,** *249,* 155–162.

46. Kouwatli, H.; Chalom, J.; Tod, M.; Farinotti, R.; Mahuzier, G. *Anal. Chim. Acta.* **1992,** *266,* 243–249.

47. Lewis, S.; Price, D.; Worsfold, P. *J. Biolum. Chemilum.* **1993,** *8(4),* 183–199.

48. Nishitani, A.; Kanda, S.; Imai, K. *Biomed. Chrom.* **1992,** *6(3),* 124–127.

49. Gübitz, G.; Zoonen, P. V.; Gooijer, C.; Velthorst, N. H.; Frei, R. W. *Anal. Chem.* **1985,** *57(11),* 2071–2074.

50. Zoonen, P. V.; Kamminga, D. A.; Gooijer, C.; Velthorst, N. H.; Frei, R. W. *Anal. Chim. Acta.* **1985,** *174,* 151–161.

51. Stigbrand, M.; Ponten, E.; Irgum, K. *Anal. Chem.* **1994,** *66(10),* 1766–1770.

52. Nakashima, K.; Wada, M.; Kuroda, N.; Akiyama, S.; Imai, K. *J. Liq. Chromatogr.* **1994,** *17(10),* 2111–2126.

53. Ponten, E.; Stigbrand, M.; Irgum, K. *Anal. Chem.* **1995,** *67(23),* 4302–4308.

54. Williams, D. C.; Huff, G. F.; Seitz, W. R. *Anal. Chem.* **1976,** *48(7),* 1003–1006.

55. Seitz, W. R., Chemiluminescence of enzymically generated peroxide, in *Bioluminescence and Chemiluminescence*; M. A. DeLuca, Ed.; Academic Press: New York, 1978; pp 456–462.

56. Rigin, V. I. *Zh. Anal. Khim.* **1978,** *23(8),* 1623–1630.

57. Rigin, V. I. *Zh. Anal. Khim.* **1979,** *34(4),* 799–804.

58. Rigin, V. I. *Zh. Anal. Khim.* **1981,** *36(8),* 1582–1587.

59. Rigin, V. I. *Zh. Anal. Khim.* **1982,** *37(9),* 1676–1681.

60. Rigin, V. I. *Zh. Anal. Khim.* **1983,** *38(9),* 1730–1733.

61. Abdel-Latif, M. S.; Guibault, G. G. *Anal. Chem.* **1988,** *60(24),* 2671–2674.

62. Kojo, S.; Tokumaru, S.; Kishida, E. *Clin. Chem.* **1992,** *38(5),* 788.

63. Nakashima, K.; Kuroda, N.; Kawaguchi, S.; Wada, M.; Akiyama, S. *J. Biolumin. Chemilumin.* **1995,** *10(3),* 185–191.

64. Grayeski, M. L.; Seitz, W. R. *Anal. Biochem.* **1984,** *136,* 277–284.

65. Arakawa, H.; Maeda, M.; Tsuji, A. *Clin. Chem.* **1985,** *31(3),* 430–434.

66. Takayasu, S.; Maeda, M.; Tsuji, A. *J. Immunol. Methods.* **1985,** *83,* 317–325.

67. Albrecht, S.; Brandl, H.; Böhm, W.-D.; Beckert, R.; Kroschwitz, H.; Neumeister, V. *Anal. Chim. Acta.* **1991,** *255,* 413-416.

68. Albrecht, S.; Hornak, H.; Freidt, T.; Bohm, W.; Weis, K.; Reinschke, A. *J. Biolum. Chemilum.* **1993,** *8(1),* 21–24.

69. Chimeno, J.; Wandruszka, R. V. *Anal. Lett.* **1989,** *22(9),* 2059–2064.

70. Abubaker, M. A.; Wandruszka, R. V. *Anal. Lett.* **1991,** *24(1),* 93–102.

71. Zoonen, P. V.; Bock, H.; Gooijer, C.; Velthorst, N. H.; Frei, R. W. *Anal. Chim. Acta.* **1987,** *200,* 131–141.

72. Gooijer, C.; Zoonen, P. V.; Velthorst, N. H.; Frei, R. W. *J. Biolum. Chemilum.* **1989,** *4,* 479–483.

73. Gooijer, C.; Velthorst, N. H. *Biomed. Chrom.* **1990,** *4(3),* 92–95.

74. DeVasto, K. K.; Grayeski, M. L. *Analyst,* **1991,** *116(5),* 443–447.

75. Holzbecher, Z.; Kábrt, L.; Jansta, L. *Coll. Czech. Chem. Commun.* **1982,** *47,* 1606–1612.

76. deLavalle, R.; Grayeski, M. L. *Anal. Biochem.* **1991,** *197,* 340–346.

77. Cepas, J.; Silva, M.; Perezbendito, D. *Anal. Chim. Acta.* **1995,** *314(1–2),* 87–94.

78. Katayama, M.; Taniguchi, H.; Matsuda, Y.; Akihama, S.; Hara, I.; Sato, H.; Kaneko, S.; Kuroda, Y.; Nozawa, S. *Anal. Chim. Acta.* **1995,** *303(2–3),* 333–340.

79. Capomacchia, A. C.; Jennings, R. N.; Hemingway, S. M.; D'Souza, P.; Prapaitrakul, W.; Gingle, A. *Anal. Chim. Acta.* **1987,** *196,* 305–310.

80. Imai, K.; Weinberger, R. *Trends Anal. Chem.* **1985,** *4(7),* 170–175.

81. de Jong, G.; Kwakman, P. J. *Chrom. Biomed. Appl.* **1989,** *492(Aug.),* 319–343.

82. Givens, R. S.; Schowen, R. L., The Peroxyoxalate Chemiluminescence Reaction, *in Photochemical Reaction Detection, in Chromatography,* J. W. Birks, Ed.; VCH: New York, 1989; pp 125–147.

83. de Jong, G. J.; Lammers, N.; Spruit, F. J.; Brinkman, U. A. T.; Frei, R. W. *Chromatographia,* **1984,** *18(3),* 129–133.

84. Grayeski, M. L.; Weber, A. J. *Anal. Lett.* **1984,** *17(A13),* 1539–1552.

85. Kobayashi, S.; Imai, K. *Anal. Chem.* **1980,** *52,* 1548–1549.

86. Scholten, A.; Brinkman, U.; Frei, R. *J. Chromatography,* **1981,** *218(1–3),* 3–13.

87. Miyaguchi, K.; Honda, K.; Imai, K. *J. Chromatography,* **1984,** *316,* 501–505.

88. Weinberger, R.; Mannan, C. A.; Cerchio, M.; Grayesky, M. L. *J. Chromatography,* **1984,** *288,* 445–450.

89. Mann, B.; Grayeski, M. L. *Anal. Chem.* **1990,** *62(14),* 1532–1536.

90. Cepas, J.; Silva, M.; Perezbendito, D. *Anal. Chem.* **1995,** *67(23),* 4376–4379.

91. Hanaoka, N.; Tanaka, H.; Nakatomo, A.; Takada, M. *Anal. Chem.* **1991,** *63(23),* 2680–2685.

92. Sherman, P. A.; Holzbecher, J.; Ryan, D. E. *Anal. Chim. Acta.* **1978,** *97,* 21–27.

93. Rigin, V. I. *Zh. Anal. Khim.* **1979,** *34(4),* 680–686.

94. Kobayashi, S.; Imai, K. *Anal. Chem.* **1980,** *52(3),* 424–427.

95. Weinberger, R. *J. Chromatography,* **1984,** *314,* 155–165.

96. Honda, K.; Miyaguchi, K.; Imai, K. *Anal. Chim. Acta.* **1985,** *177,* 103–110.

97. Nakashima, K.; Maki, K.; Akiyama, S.; Wang, W. H.; Tsukamoto, Y.; Imai, K. *Analyst,* **1989,** *114(11),* 1413–1416.

98. Milofsky, R. E.; Birks, J. W. *Anal. Chem.* **1990,** *65(10),* 1050–1054.

99. Steijger, O. M.; Rodenburg, P. H. M.; Lingeman, H.; Brinkman, U. A. T.; Holthuis, J. J. M. *Anal. Chim. Acta.* **1992,** *266,* 233–241.

100. Sugiura, M.; Kanda, S.; Imai, K. *Anal. Chim. Acta.* **1992,** *266,* 225–231.

101. de Jong, G. J.; Lammers, N.; Spruit, F. J.; Frei, R. W.; Brinkman, U. A. T. *J. Chrom.* **1986,** *353,* 249–257.

102. Hanaoka, N.; Givens, R. S.; Schowen, R. L.; Kuwana, T. *Anal. Chem.* **1988,** *60(20),* 2193–2197.

103. Bryan, P. D.; Capomacchia, A. C. *J. Pharm. Biomed. Anal.* **1991,** *9(10–12),* 855–860.

104. Orlovic, M.; Schowen, R. L.; Givens, R. S.; Alvarez, F.; Matuszewski, B.; Parekh, N. J. *Org. Chem.* **1989,** *54,* 3606–3610.

105. Catherall, C. L. R.; Palmer, T. F.; Cundall, R. B. *J. Chem. Soc., Faraday Trans. 2.* **1984,** *80,* 823–836.

106. Catherall, C. L. R.; Palmer, T. F.; Cundall, R. B. *J. Chem. Soc., Faraday Trans. 2.* **1984,** *80,* 837–849.

107. Orosz, G. *Tetrahedron,* **1989,** *45(11),* 3493–3506.

108. Hanaoka, N. *J. Chrom.* **1990,** *503,* 155–165.

109. Oh, S.; Cha, S. *Anal. Biochem.* **1994,** *218(1),* 222–224.

110. Steijger, O. M.; Mastbergen, H. M. V.; Holthius, J. J. M. *Anal. Chim. Acta.* **1989,** *217,* 229–237.

111. Dan, N.; Lau, M. L.; Grayeski, M. L. *Anal. Chem.* **1991,** *63,* 1766–1771.

112. Jennings, R. N.; Capomacchia, A. C. *Anal. Chim. Acta.* **1988,** *205,* 207–213.

113. Orosz, G.; Dudar, E. *Anal. Chim. Acta.* **1991,** *247,* 141–147.

114. Neuvonen, H. *J. Chem. Soc., Perkin Trans. 2.* **1994,** *1,* 89–95.

115. Neuvonen, H. J. *Chem. Soc., Perkin Trans. 2.* **1995,** *5,* 945–949.

116. Milofsky, R. E.; Birks, J. W. *J. Am. Chem. Soc.* **1991,** *113(26),* 9715–9723.

117. Alvarez, F. J.; Parekh, N. J.; Matuszewski, B.; Givens, R. S.; Higuchi, T.; Schowen, R. L. *J. Am. Chem. Soc.* **1986,** *108(20),* 6435–6437.

118. Chokshi, H. P.; Barbush, M.; Carlson, R. G.; Givens, R. S.; Kuwana, T.; Schowen, R. L. *Biomed. Chrom.* **1990,** *4(3),* 96–99.

119. Rauhut, M. M. *Acc. Chem. Res.* **1969,** *2(3),* 81–87.

120. Rauhut, M. M.; Bollyky, L. J.; Roberts, B. G.; Loy, M.; Whitman, R. H.; Ianotta, A. V.; Semsel, A. M.; Clarke, R. A. *J. Am. Chem. Soc.* **1967,** *89(25),* 6515–6522.

121. Prados, P.; Santa, T.; Homma, H.; Imai, K. *Anal. Sci.* **1995,** *11(4),* 575–580.

122. Schuster, G. B.; Schmidt, S. P., Chemiluminescence of Organic Compounds, in *Advances in Physical Organic Chemistry,* V. Gold and D. Bethell, Eds.; Academic Press: New York, 1982; pp 187–238.

123. Milas, N. A.; Panagiotakos, P. C. *J. Am. Chem. Soc.* **1946,** *68,* 533–534.

124. Kang, S. C.; Lee, S. K.; Song, H.-S.; Kim, K.-J. *Bull. Korean Chem. Soc.* **1989,** *10(4),* 408–409.

125. Orosz, G.; Givens, R. S.; Schowen, R. L. *Anal. Chim. Acta.* **1992,** *266(2),* 219–223.

126. Orosz, G.; Torkos, K.; Borossay, J. *Acta Chim. Hungarica,* **1991,** *128(6),* 911–917.

127. Honda, K.; Miyaguchi, K.; Imai, K. *Anal. Chim. Acta.* **1985,** *177,* 111–120.

128. Tod, M.; Farinotti, R.; Mahuzier, G.; Gaury, I. *Anal. Chim. Acta.* **1989,** *217,* 11–21.